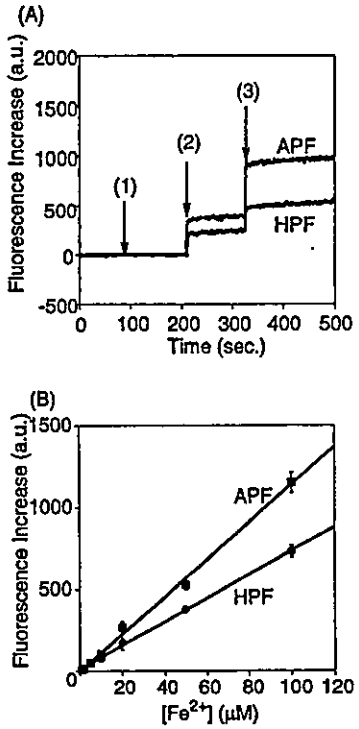

FIG. 2. **Detection of 'OH in the Fenton reaction using HPF and APF.** *A*, HPF (*lower line*) or APF (*upper line*) (final 10 μM; 0.1% DMF as a cosolvent) were added to sodium phosphate buffer (0.1 M, pH 7.4). The fluorescence intensity was determined at 515 nm with excitation at 490 nm. H_2O_2 (final 1 mM) was added at *1*, and ferrous perchlorate (final 100 μM) was added two times at *2* and *3*. *B*, relation between the concentrations of added ferrous perchlorate and fluorescence increase in the Fenton reaction. Data are mean ± S.E. (n = 3). HPF (*circle*) or APF (*square*) (final 10 μM; 0.1% DMF as a cosolvent) were added to sodium phosphate buffer (0.1 M, pH 7.4) containing H_2O_2 (1 mM). The wavelength for measurement was the same as *A*.

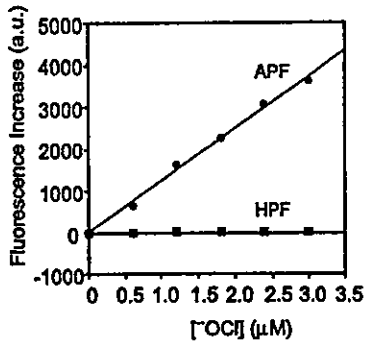

FIG. 3. **Detection of $^-$OCl by HPF and APF.** Relation between the concentrations of added NaOCl and fluorescence increase. HPF (*square*) or APF (*circle*) (final 10 μM; 0.1% DMF as a cosolvent) were added to sodium phosphate buffer (0.1 M, pH 7.4). The fluorescence intensity was determined at 515 nm with excitation at 490 nm.

TABLE I
Fluorescence increase of HPF, APF, and DCFH in various ROS generating systems

Dyes (final 10 μM, 0.1% DMF as a cosolvent) were added to sodium phosphate buffer (0.1 M, pH 7.4). The fluorescence intensities of HPF, APF, and DCFH were measured at 515, 515, and 520 nm with excitation at 490, 490, and 500 nm, respectively. DCFH was obtained by the hydrolysis of DCFH-DA with base as mentioned under "Experimental Procedures."

ROS	HPF	APF	DCFH
'OH[a]	730	1200	7400
$ONOO^-$[b]	120	560	6600
^-OCl[c]	6	3600	86
$^1O_2$[d]	5	9	26
$O_2^{\cdot-}$[e]	8	6	67
H_2O_2[f]	2	<1	190
NO[g]	6	<1	150
ROO'[h]	17	2	710
Autoxidation[i]	<1	<1	2000

[a] Ferrous perchlorate (100 μM) and H_2O_2 (1 mM) were added at room temperature.
[b] $ONOO^-$ (final 3 μM) was added at 37 °C.
[c] NaOCl (final 3 μM) was added at 37 °C.
[d] 3-(1,4-Dihydro-1,4-epidioxy-1-naphthyl)propionic acid (100 μM) was added and the mixtures were stirred at 37 °C for 30 min.
[e] KO_2 (100 μM) was added and the mixtures were stirred at 37 °C for 30 min.
[f] H_2O_2 (100 μM) was added and the mixtures were stirred at 37 °C for 30 min.
[g] 1-Hydroxy-2-oxo-3-(3-aminopropyl)-3-methyl-1-triazene (100 μM) was added and the mixtures were stirred at 37 °C for 30 min.
[h] 2,2'-Azobis(2-amidinopropane)dihydrochloride (100 μM) was added and the mixtures were stirred at 37 °C for 30 min.
[i] Dye solutions were placed under a fluorescent lamp for 2.5 h.

raphy and three-dimensional fluorescence spectroscopy (data not shown). Furthermore, we examined the relation between the concentration of ferrous perchlorate and the fluorescence increase in the Fenton reaction (Fig. 2*B*). Ferrous perchlorate was added at various concentrations to buffer solutions of HPF and APF containing an excess of H_2O_2. The results showed that the fluorescence increase is proportional to the concentration of ferrous perchlorate. Therefore, both HPF and APF can detect 'OH formed in the Fenton reaction in terms of a dose-dependent increase of fluorescence.

Reactivity of HPF and APF with ^-OCl—$^-$OCl has a strong microbicidal activity, and plays a key role in the killing of bacteria by neutrophils (29, 30). Therefore, we investigated the reactivity of HPF and APF with $^-$OCl. The results are shown in Fig. 3. Interestingly, the fluorescence intensity of APF greatly increased upon addition of $^-$OCl, whereas that of HPF did not. In addition, the fluorescence increase of APF was dose-dependent. Therefore, we could detect $^-$OCl selectively by using both HPF and APF together.

Reactivity of HPF, APF, and DCFH with Various ROS, and the Lability of the Probes to Light-induced Autoxidation—As mentioned above, DCFH is widely used as a fluorescence probe for ROS, but it lacks specificity among ROS and suffers from autoxidation; that is, the fluorescence increases even in the absence of ROS upon illumination. We compared the reactivities of HPF, APF, and DCFH with $O_2^{\cdot-}$, H_2O_2, 'OH, $^1O_2$, $^-$OCl, NO, peroxynitrite ($ONOO^-$), and alkylperoxyl radical (ROO'). The observed fluorescence increases are shown in Table I. 3-(1,4-Dihydro-1,4-epidioxy-1-naphthyl)propionic acid thermally generates $^1O_2$ under mild conditions (31) and 1-hydroxy-2-oxo-3-(3-aminopropyl)-3-methyl-1-triazene thermally generates NO· under mild conditions (32). 2,2'-Azobis(2-amidinopropane)dihydrochloride is an azo-initiator that forms alkyl radicals as a result of thermal decomposition, and these alkyl radicals can react with molecular oxygen to give alkylperoxyl radicals (33). Under these conditions, DCFH reacted unselectively with all of these reactive species. On the other hand, HPF and APF showed fluorescence augmentation only upon reaction with 'OH, $ONOO^-$, and/or $^-$OCl, and not with $O_2^{\cdot-}$, H_2O_2, $^1O_2$, NO, ROO', which are thought to be produced in many biological systems. $ONOO^-$ has a strong oxidizing power (34, 35), so it should be included in the category of hROS. Furthermore, DCFH was extensively autoxidized, resulting in a marked increase of the fluorescence intensity, whereas HPF and APF were not autoxidized at all. These results show that HPF and APF have much higher selectivity among ROS and a greater resistance to autoxidation than DCFH.

Next, we examined whether light-induced autoxidation would occur under conditions practically used for excitation in

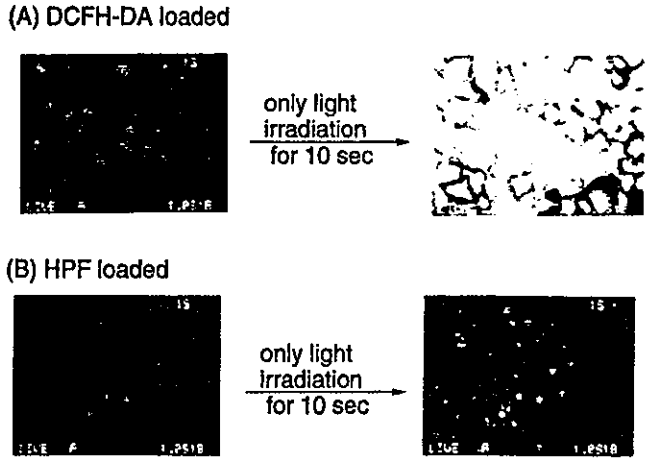

FIG. 4. **Light-induced autoxidation in DCFH-DA-loaded HLE cells (*A*) and HPF-loaded HLE cells (*B*).** HLE cells were loaded with DCFH-DA or HPF (10 μM; 0.1% DMF as a cosolvent) by incubation for 30 min at 37 °C in the dark. Fluorescence images were acquired. After that, the cells were laser-irradiated at 488 nm for 10 s, and fluorescence images were acquired again.

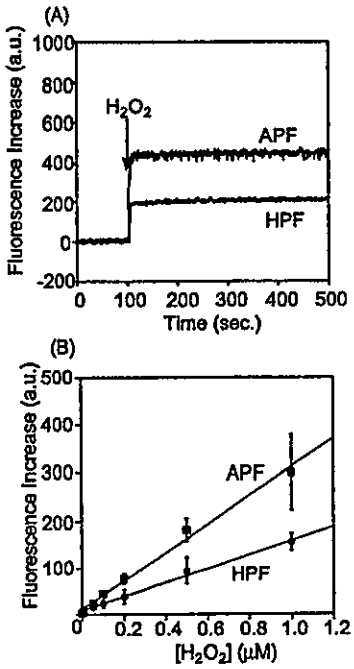

FIG. 5. **Detection of hROS in the HRP/H_2O_2 system using HPF and APF.** *A*, representative data are shown (n = 3). HPF (*lower line*) or APF (*upper line*) (final 10 μM; 0.1% DMF as a cosolvent) were added to sodium phosphate buffer (0.1 M, pH 7.4) containing HRP (0.2 μM). H_2O_2 (final 1 μM) was added at the time indicated by the *arrow*. The fluorescence intensity was determined at 515 nm with excitation at 490 nm. These reactions were performed at 37 °C. *B*, relation between the amount of added H_2O_2 and fluorescence increase in the HRP/H_2O_2 system using HPF (*circle*) and APF (*square*). Data are mean ± S.E. (n = 3). Dyes (final 10 μM; 0.1% DMF as a cosolvent) were added to sodium phosphate buffer (0.1 M, pH 7.4) containing HRP (0.2 μM). The fluorescence intensity was determined at 515 nm with excitation at 490 nm. These reactions were performed at 37 °C for 5 min.

fluorescence microscopy. We loaded HPF or DCFH-DA into HLE cells and irradiated the dye-loaded cells for 10 s. Fluorescein and dichlorofluorescein, the autoxidized products, form dianions in the buffer (pH 7.3) (36, 37), and therefore tend to remain in the intracellular medium. The results are shown in Fig. 4. HPF could permeate the cell membrane and enter into cells. DCFH was much more easily autoxidized by light irradiation than HPF in cells under conditions practically used for excitation in fluorescence microscopy.

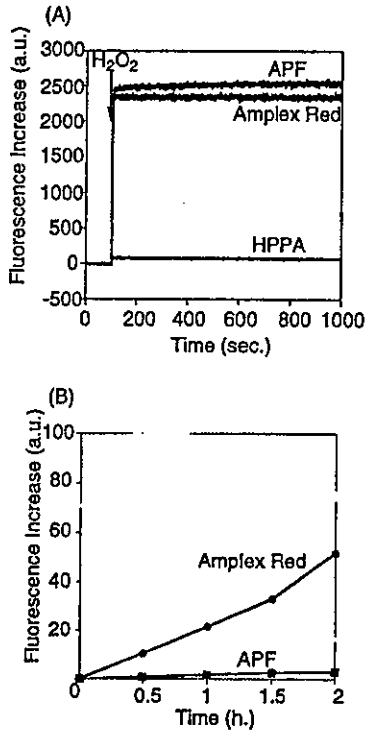

FIG. 6. **Comparison between APF, Amplex Red, and HPPA.** *A*, comparison of the sensitivity in the HRP/H_2O_2 system. Dyes (final 10 μM; 0.1% DMF as a cosolvent) were added to 0.15 M KCl, 25 mM Tris-HCl buffer (pH 7.4) containing HRP (0.2 μM). H_2O_2 (final 3 μM) was added at the time indicated by the *arrow*. The fluorescence intensity with APF, Amplex Red, and HPPA was determined at 515, 580, and 405 nm with excitation at 490, 570, and 320 nm, respectively. These reactions were performed at 37 °C. *B*, comparison of the lability of light-induced autoxidation. Dyes (final 10 μM; 0.1% DMF as a cosolvent) were added to 0.15 M KCl, 25 mM Tris-HCl buffer (pH 7.4). Dyes were placed under a fluorescent lamp for the indicated time.

Application of HPF and APF to an Enzymatic System—We investigated whether HPF and APF could detect hROS generated in an enzymatic system, *i.e.* the HRP/H_2O_2 system. In this system, two-electron oxidation of the native enzyme (HRP) to compound I is followed by two one-electron reductions to yield the resting state of HRP (38). H_2O_2 was added to buffer solutions of HPF and APF containing HRP. As shown in Fig. 5*A*, the fluorescence intensity increased immediately upon the addition of H_2O_2. Furthermore, it was found that HPF and APF could detect hROS generated in the HRP/H_2O_2 system in a dose-dependent manner (Fig. 5*B*). Thus, the data in Fig. 5 really show that HPF and APF can serve as substrates for horseradish peroxidase, and HPF and APF could detect hROS in a dose-dependent manner not only in a chemical system, but also in an enzymatic system.

Next, we compared the reactivity for hROS generated in the HRP/H_2O_2 system and the lability to light-induced autoxidation among our novel fluorescence probe APF and two widely used fluorescence probes for peroxidase (Amplex Red and HPPA) (39, 40). APF had slightly greater reactivity than Amplex Red for hROS generated in the HRP/H_2O_2 system and much greater reactivity than HPPA (Fig. 6*A*). Furthermore, APF had much greater resistance to autoxidation than Amplex Red (Fig. 6*B*). Therefore, APF is superior to the most widely used fluorescence probes for peroxidase.

Furthermore, we applied HPF and APF to the MPO/H_2O_2/Cl^- system. In the presence of Cl^-, ^-OCl is predominantly produced via the reactive intermediate, compound I. The re-

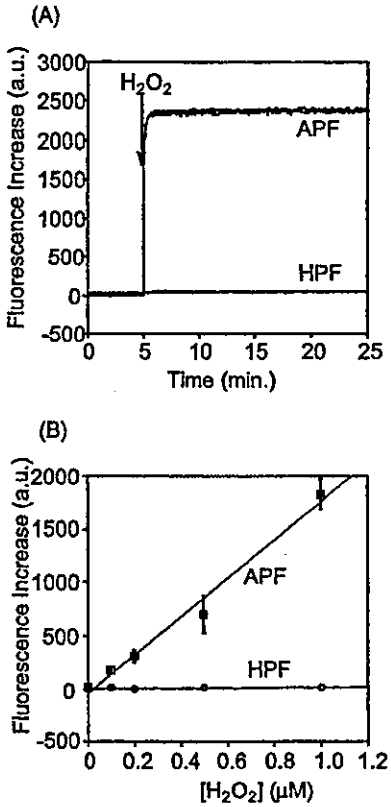

FIG. 7. **Application of HPF and APF to the MPO/H_2O_2/Cl^- system.** *A*, representative data are shown (n = 3). HPF (*lower line*) or APF (*upper line*) (final 10 μM; 0.1% DMF as a cosolvent) were added to sodium phosphate buffer (0.1 M, pH 7.4) containing MPO (11.2 nM) and NaCl (150 mM). H_2O_2 (final 1 μM) was added at the time indicated by the *arrow*. The fluorescence intensity was determined at 515 nm with excitation at 490 nm. These reactions were performed at 37 °C. *B*, relation between the amount of added H_2O_2 and fluorescence increase in the MPO/H_2O_2/Cl system using HPF (*circle*) and APF (*square*). Data are mean ± S.E. (n = 3). The buffer and wavelength for measurement were same as *A*. These reactions were performed at 37 °C for 25 min.

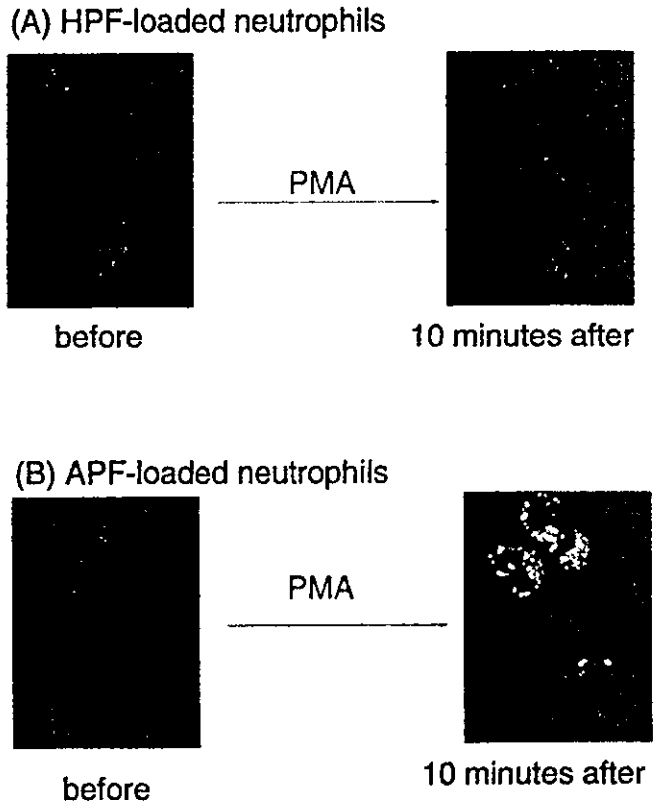

FIG. 8. **Fluorescence images of HPF- or APF-loaded neutrophils.** HPF or APF (final 10 μM; 0.1% DMF as a cosolvent) were loaded into neutrophils for 30 min at room temperature, and the dye-loaded neutrophils were stimulated with PMA (2 ng/ml). Fluorescence images were acquired before and 10 min after the stimulation with PMA.

sults are shown in Fig. 7. APF showed a dose-dependent fluorescence increase in this system, whereas HPF showed no fluorescence. These results correspond well with the reactivities of HPF and APF for $^{\cdot}OCl$. Therefore, we succeeded in visualizing the production of $^{\cdot}OCl$ in the MPO/H_2O_2/Cl^- system.

Application of HPF and APF to Neutrophils—Neutrophils are a population of circulating blood cells, and their primary function is host defense against pathogenic microorganisms. Exposure of neutrophils to various stimuli such as PMA (41) and fatty acids (42) activates the "respiratory burst oxidase," NADPH oxidase, to generate $O_2^{\cdot-}$, which is then converted to H_2O_2 and O_2 (43, 44). As neither $O_2^{\cdot-}$ nor H_2O_2 is strongly microbicidal, these species are thought to be precursors of more potent oxidizing agents, such as $^{\cdot}OH$, ^{-}OCl, and $^1O_2$. Neutrophils contain azurophilic granules, in which MPO exists abundantly, and MPO has been shown to catalyze the formation of ^{-}OCl from H_2O_2 and Cl^- *in vitro* (45). Therefore, we tried to apply our novel fluorescence probes to neutrophils. We stimulated HPF- or APF-loaded neutrophils with PMA, and observed the dye-loaded neutrophils without washing out the extracellular medium. The results are shown in Fig. 8. It is noteworthy that the fluorescence intensity of HPF-loaded neutrophils did not change upon stimulation with PMA, whereas that of APF-loaded neutrophils greatly increased. Our results suggest that MPO produces ^{-}OCl in the presence of both Cl^- and H_2O_2, which is generated by the stimulation with PMA, and we could identify this ^{-}OCl production by using HPF and APF together. In other words, we could for the first time visualize $^{\cdot}OCl$ selectively, distinguishing it from other ROS, by using HPF and APF together, even in a biological system.

DISCUSSION

We have succeeded in developing novel autoxidation-resistant fluorescence probes, HPF and APF, that can reliably detect hROS and/or ^{-}OCl selectively. Because it is likely that individual ROS have distinct roles in biological systems, the availability of selective fluorescence probes will be extremely useful. For example, by using HPF or APF, we can distinguish $^{\cdot}OH$ from NO. This is very important, because DCFH reacts with both $^{\cdot}OH$ and NO and so cannot be used reliably to study the biological role of $^{\cdot}OH$. In addition, the mere production of H_2O_2 is completely different in terms of cell damage from the situation in which H_2O_2 is converted into hROS in the presence of low-valent metal ions. We feel our probes are useful here, because they can distinguish these two situations. Furthermore, we can also distinguish $ONOO^-$ from NO or $O_2^{\cdot-}$. It has been reported that $ONOO^-$ can be generated from NO and $O_2^{\cdot-}$ *in vitro* and *in vivo* (46, 47), and therefore we will be able to visualize the production of $ONOO^-$ with a clear distinction from that of NO or $O_2^{\cdot-}$, and this will allow a reliable evaluation of the role of $ONOO^-$ in various processes. Furthermore, we could detect $^{\cdot}OCl$ selectively by using HPF and APF together, because HPF shows no fluorescence increase with ^{-}OCl, whereas APF shows a dose-dependent increase. The ability to selectively detect individual species of ROS represents a major advance.

As shown in Table I and Fig. 4, the currently used fluorescence probe DCFH is easily autoxidized by light irradiation. This means that precautions must be taken to exclude light during incubation to load DCFH-DA into cells, and it is neces-

sary to change the visual field often during observations. However, HPF and APF are not autoxidized at all, as shown in Table I and Fig. 4. Therefore, we believe HPF and APF will contribute greatly to the elucidation of the roles of ROS in living cells by making it possible to see the generation of specific ROS with high resolution in time and space. Although the sensitivity of HPF and APF is inferior to that of DCFH (Table I), lability to autoxidation and selectivity among ROS, rather than sensitivity, are considered to be critical for fluorescence probes for ROS.

The question arises, why are HPF and APF selective for hROS, unlike DCFH? DCFH is nonfluorescent, and HPF and APF possess low fluorescence quantum efficiency, and all of them are converted to strongly fluorescent compounds, dichlorofluorescein or fluorescein, by oxidation. However, DCFH is converted to dichlorofluorescein, initially via abstraction of the hydrogen atom at the 9′-position, whereas HPF and APF are converted to fluorescein, initially via abstraction of the hydrogen atom of the phenolic hydroxy group or abstraction of one electron from the nitrogen atom. The hydrogen atom at the 9′-position of DCFH is readily abstracted because this hydrogen atom can be considered as being located at the central carbon of a triphenylmethane. It is therefore vulnerable even to a weakly oxidizing species, and this is the reason why DCFH lacks the selectivity among ROS. However, a strongly oxidizing species is required for the *ipso*-substitution reaction of HPF and APF. Therefore, we conclude that the difference of oxidizing power required for oxidation reaction used for detection causes the difference of selectivity among ROS. Furthermore, the fact that HPF shows no fluorescence increase with $^{-}$OCl, whereas APF does (Fig. 3 and Table I), reflects the difference in lability to oxidation between an aryloxyphenol and an aryloxyaniline.

HPF and APF could detect hROS generated in the HRP/H_2O_2 system (Fig. 5). HRP is often used as an enzyme label in immunohistochemical studies, 3,3-diaminobenzidine is commonly used as a substrate for measurement of the peroxidase activity. However, 3,3-diaminobenzidine can be detected only by absorbance measurement and is easily autoxidized by light irradiation. Because HPF and APF permit fluorescence detection, which has higher sensitivity than absorbance detection, and they are not autoxidized by light irradiation at all, they are likely to be more effective reagents for immunohistochemistry using peroxidase than 3,3-diaminobenzidine and related compounds.

We also used HPF and APF to visualize the production of $^{-}$OCl from neutrophils (Fig. 8). Dye-loaded neutrophils weakly fluoresced before the stimulation with PMA, because the dyes were taken up by pinocytosis and MPO was slightly released into pinocytic vacuoles. Nevertheless, the fluorescence intensity of APF-loaded neutrophils markedly increased, in contrast to little fluorescence increase of HPF-loaded cells upon stimulation with PMA. $^{-}$OCl is believed to play important roles not only in bacterial killing bacteria by neutrophils but also in injury to the venular endothelial surface in platelet-activating factor-induced microvascular damage (48). However, it has been difficult to draw firm conclusions concerning direct participation of $^{-}$OCl because a completely selective detection method for $^{-}$OCl has never been developed. Therefore, our finding that we could detect $^{-}$OCl selectively by using HPF and APF together will make it possible for the first time to elucidate reliably the roles of $^{-}$OCl in biological systems such as neutrophils.

In summary, we have developed novel fluorescence probes, HPF and APF, that can selectively and dose dependently detect certain species among ROS and that are highly resistant to autoxidation. They can be used in enzymatic and cellular systems. They are greatly superior to the existing fluorescence probes for ROS, and are expected to have many chemical and biological applications.

Acknowledgment—We thank Dr. Hidehiko Nakagawa (National Institute of Radiological Sciences, Chiba, Japan) for providing peroxynitrite solution.

REFERENCES

1. Wiseman, H., and Halliwell, B. (1996) *Biochem. J.* **313**, 17–29
2. McCord, J. M. (1974) *Science* **185**, 529–531
3. Dobashi, K., Ghosh, B., Orak, J. K., Singh, I., and Singh, A. K. (2000) *Mol. Cell. Biochem.* **205**, 1–11
4. Schmidt, K. N., Amstad, P., Cerutti, P., and Baeuerle, P. A. (1995) *Chem. Biol.* **2**, 13–22
5. Yermolaieva, O., Brot, N., Weissbach, H., Heinemann, S. H., and Hoshi, T. (2000) *Proc. Natl. Acad. Sci. U. S. A.* **97**, 448–453
6. Frohlich, K. U., and Madeo, F. (2000) *FEBS Lett.* **473**, 6–9
7. Nishida, M., Maruyama, Y., Tanaka, R., Kontani, K., Nagao, T., and Kurose H. (2000) *Nature* **408**, 492–495
8. Kuppusamy, P., Chzhan, M., Vij, K., Shteynbuk, M., Lefer, D. J., Giannella, E., and Zweier, J. L. (1994) *Proc. Natl. Acad. Sci. U. S. A.* **91**, 3388–3392
9. Yasui, H., and Sakurai, H. (2000) *Biochem. Biophys. Res. Commun.* **269**, 131–136
10. Grynkiewicz, G., Poenie, M., and Tsien, R. Y. (1985) *J. Biol. Chem.* **260**, 3440–3450
11. Minta, A., Kao, J. P. Y., and Tsien, R. Y. (1989) *J. Biol. Chem.* **264**, 8171–8178
12. Hempel, S. L., Buettner, G. R., O'Malley, Y. Q., Wessels, D. A., and Flaherty, D. M. (1999) *Free Radical Biol. Med.* **27**, 146–159
13. Matoba, T., Shimokawa, H., Nakashima, M., Hirakawa, Y., Mukai, Y., Hirano, K., Kanaide, H., and Takeshita, A. (2000) *J. Clin. Invest.* **106**, 1521–1530
14. Zhuang, S. G., Demirs, J. T., and Kochevar, I. E. (2000) *J. Biol. Chem.* **275**, 25939–25948
15. Tatla, S., Woodhead, V., Foreman, J. C., and Chain, B. M. (1999) *Free Radical Biol. Med.* **26**, 14–24
16. Umezawa, N., Tanaka, K., Urano, Y., Kikuchi, K., Higuchi, T., and Nagano, T. (1999) *Angew. Chem. Int. Ed.* **38**, 2899–2901
17. Coudray, C., and Favier, A. (2000) *Free Radical Biol. Med.* **29**, 1064–1070
18. Grishko, V. I., Druzhyna, N., LeDoux, S. P., and Wilson, G. L. (1999) *Nucleic Acids Res.* **27**, 4510–4516
19. Rota, C., Fann, Y. C., and Mason, R. P. (1999) *J. Biol. Chem.* **274**, 28161–28168
20. Rota, C., Chignell, C. F., and Mason, R. P. (1999) *Free Radical Biol. Med.* **27**, 873–881
21. Ren, J.-G., Xia, H.-L., Just, T., and Dai, Y.-R. (2001) *FEBS Lett.* **488**, 123–132
22. Az-ma, T., Saeki, N., and Yuge, O. (1999) *Br. J. Pharmacol.* **126**, 1462–1470
23. Motoori, S., Majima, H. J., Ebara, M., Kato, H., Hirai, F., Kakinuma, S., Yamaguchi, C., Ozawa, T., Nagano, T., Tsujii, H., and Saisho, H. (2001) *Cancer Res.* **61**, 5382–5388
24. Wakeyama, H., Takeshige, K., Takayanagi, R., and Minakami, S. (1982) *Biochem. J.* **205**, 593–601
25. Kakinuma, K., Kaneda, M., Chiba, T., and Ohnishi, T. (1986) *J. Biol. Chem.* **261**, 9426–9432
26. Böyum, A. (1968) *Scand. J. Clin. Lab. Invest.* **21**, 77–98
27. Ohe, T., Mashino, T., and Hirobe, M. (1995) *Tetrahedron Lett.* **36**, 7681–7684
28. Urano, Y., Higuchi, T., and Hirobe, M. (1996) *J. Chem. Soc. Perkin Trans.* **2**, 1169–1173
29. Smith, J. A., and Weidemann, M. J. (1993) *J. Immunol. Methods* **162**, 261–268
30. Samuni, A., Krishna, C. M., Cook, J., Black, C. D. V., and Russo, A. (1991) *Free Radical Biol. Med.* **10**, 305–313
31. Aubry, J. M., Cazin, B., and Duprat, F. (1989) *J. Org. Chem.* **54**, 726–728
32. Hrabie, J. A., Klose, J. R., Wink, D. A., and Keefer, L. K. (1993) *J. Org. Chem.* **58**, 1472–1476
33. Damiani, E., Kalinska, B., Canapa, A., Canestrari, S., Wozniak, M., Olmo, E., and Greci, L. (2000) *Free Radical Biol. Med.* **28**, 1257–1265
34. Halfpenny, E., and Robinson, P. L. (1952) *J. Chem. Soc.* 939–946
35. Beckman, J. S., Beckman, T. W., Chen, J., Marshall, P. A., and Freeman, B. A. (1990) *Proc. Natl. Acad. Sci. U. S. A.* **87**, 1620–1624
36. Tamura, Z., Morioka, T., Maeda, M., and Tsuji, A. (1994) *Bunseki Kagaku* **43**, 339–346
37. Mchedlovpetrossyan, N. O., Rubtsov, M. I., and Lukatskaya, L. L. (1992) *Dyes Pigments* **18**, 179–198
38. Rodríguez-López, J. N., Lowe, D. J., Hernández-Ruiz, J., Hiner, A. N. P., García-Cánovas, F., and Thorneley, R. N. F. (2001) *J. Am. Chem. Soc.* **123**, 11838–11847
39. Raible, D. G., Mohanty, J. G., Jaffe, J. S., Stella, H. J., Sprenkle, B. E., Glaum, M. C., and Schulman, E. S. (2000) *Free Radical Biol. Med.* **28**, 1652–1660
40. Tuuminen, T., Palomaki, P., Rakkolainen, A., Welin, G., Weber, T., and Kapyaho, K. (1991) *J. Immunoassay* **12**, 29–46
41. Repine, J. E., White, J. G., Clawson, C. C., and Holmes, B. M. (1974) *J. Lab. Clin. Med.* **83**, 911–920
42. Kakinuma, K. (1974) *Biochim. Biophys. Acta* **348**, 76–85
43. Babior, B. M. (1978) *N. Engl. J. Med.* **298**, 659–668
44. Rossi, F. (1986) *Biochim. Biophys. Acta* **853**, 65–89
45. Klebanoff, S. J., and Clark, R. A. (1978) *The Neutrophils: Function and Clinical Disorders*, North-Holland Publishing Co., Amsterdam, The Netherlands
46. Blough, N. V., and Zafiriou, O. C. (1985) *Inorg. Chem.* **24**, 3502–3504
47. Xia, Y., Dawson, V. L., Dawson, T. M., Snyder, S. H., and Zweier, J. L. (1996) *Proc. Natl. Acad. Sci. U. S. A.* **93**, 6770–6774
48. Suematsu, M., Kurose, I., Asako, H., Miura, S., and Tsuchiya, M. (1989) *J. Biochem.* **106**, 355–360

Increase of Lipid Peroxidation by Cisplatin in WI38 Cells but Not in SV40-Transformed WI38 Cells

Hsiu-Chuan Yen,[1] *Chung-Yi Nien,*[1] *Hideyuki J. Majima,*[2] *Chia-Pei Lee,*[1] *Sz-Yun Chen,*[1] *Jeng-Shu Wei,*[1] *and Lai-Chu See*[3]

[1]School of Medical Technology, Chang Gung University, Kwei-Shan, Tao-Yuan 333, Taiwan, Republic of China; E-mail: *yen@mail.cgu.edu.tw*
[2]Department of Radiology, Dental School, Kagoshima University, Kagoshima 890-8544, Japan
[3]Department of Public Health, Biostatistics Consulting Center, Chang Gung University, Kwei-Shan, Tao-Yuan 333, Taiwan, Republic of China

Received 8 July 2002; revised 28 October 2002; accepted 1 November 2002

ABSTRACT: Cisplatin (CPT) is an effective anticancer drug that causes cumulative toxicity to normal tissues. It has been suggested that CPT damages normal cells by causing oxidative stress, but it is not known whether it can induce similar oxidative damage to tumor cells. In this study, by using normal human lung fibroblast (W138) cells and SV40-transformed WI38 (VA13) cells as a model, we compared the effect of CPT on cytotoxicity, apoptosis, lipid peroxidation, and mitochondrial gene expression, which could be regulated by oxidative stress, between normal and tumor cells. CPT induced greater growth inhibition and percentage of apoptotic cells in VA13 cells. However, levels of esterified F_2-isoprostanes and 4-hydroxy-2-nonenal, two specific products of lipid peroxidation, were increased by CPT in WI38 cells, but not in VA13 cells. Furthermore, the transcript level of mitochondrial 12S rRNA was augmented by CPT in both cells, but to a higher degree in WI38 cells. The data suggest a correlation between lipid peroxidation and cytotoxicity or increased mitochondrial transcript levels in WI38 cells but not in VA13 cells. The results also indicate an altered response of oxidative damage and mitochondrial gene regulation to CPT in the transformed phenotype of WI38 cells.
 J Biochem Mol Toxicol 17:39–46, 2003; Published online in Wiley InterScience (www.interscience.wiley.com). DOI 10.1002/jbt.10059

KEYWORDS: **Cisplatin; F_2-Isoprostanes; 4-Hydroxy-2-nonenal; Lipid Peroxidation; Mitochondrial Gene Expression; Transformed Cells**

INTRODUCTION

Cisplatin (CPT), or *cis*-dichlorodiammine platinum(II), is an important anticancer drug but its irreversible cumulative toxicity to normal tissue has been a major clinical problem during CPT therapy [1]. The chlorinated form of CPT becomes electrophilic once CPT gets hydrated inside the plasma membrane and can react with nucleophilic molecules such as DNA bases and sulfhydryl groups [2]. Although there is no known pathway by which CPT generates reactive oxygen species (ROS) directly, it has been proposed that oxidative stress is an important mechanism of CPT-induced normal tissue toxicity possibly due to depletion of glutathione (GSH) [2,3]. On the other hand, it has been shown that CPT inhibited the function of respiratory complexes in normal tubular cells [4]. Since mitochondrial respiratory chain is a source of ROS [5], mitochondrial damage could also be a source of oxidative stress induced by CPT. The use of antioxidants has therefore been proposed as a means to alleviate CPT-induced toxicity [6,7]. However, whether effects of CPT on redox status and mitochondria are similar between normal and tumor cells remains to be determined.

Lipid peroxidation is initiated by the abstraction of allylic hydrogen on polyunsaturated fatty acids (PUFAs) by free radicals. F_2-isoprostanes, a group of prostaglandin F_2 (PGF_2)-like compounds, are specific in vivo markers of lipid peroxidation produced from free-radical-catalyzed peroxidation of arachidonic acid independent of the cyclooxygenase pathway [8] and are initially formed in situ esterified to phospholipid on membranes [9]. 15-F_{2t}-isoprostane (15-F_{2t}-IsoP) or 8-iso-$PGF_{2\alpha}$, the most abundant form of F_2-isoprostanes in vivo, has been shown to be elevated in a variety of oxidative stress related human diseases and toxicity [10]. On the other hand, 4-hydroxy-2-nonenal (HNE) is formed during the peroxidation of ω6-PUFAs

Correspondence to: Hsiu-Chuan Yen, Ph.D.
Contract Grant Sponsor: National Science Council, Taiwan.
Contract Grant Number: NSC 89-2314-B-182-070, NSC 89-2320-B-182-053, and NSC 90-2320-B-182-061.
Contract Grant Sponsor: Ministry of Education, Culture, Sports, Science and Technology, Japan.
Contract Grant Number: JGME 12671844.

by cleavage of lipid hydroperoxides catalyzed by transition-metal ions [11]. HNE is a highly reactive and toxic aldehyde that can react with GSH or macromolecules to form protein adducts, DNA adducts, and phospholipid adducts [12]. It has been shown that HNE can modulate the activity of redox-sensitive transcription factors [13], indicating the involvement of HNE in signal transduction pathways.

Human mitochondrial DNA (mtDNA) is a circular DNA with 16,569 bp. It encodes 13 polypeptides as essential subunits of complexes for oxidative phosphorylation, and 2 rRNA and 22 tRNA genes [14]. Nuclear DNA-encoded mitochondrial transcription factor A (mtTFA) is required for the transcription of mtDNA [15]. Oxidative stress has been suggested to modulate mitochondrial gene expression either by retrograde signaling from mitochondria to nucleus or through redox-sensitive transcription factors, such as nuclear respiratory factor-2 (NRF-2), AP-1, and NF-κB [16,17]. Upregulation of both nuclear and mtDNA genes for oxidative phosphorylation was found in adenine nucleotide translocator (ANT)-1 knockout mice with oxidative stress [18,19] and in human cells treated with antimycin A that induced oxidative stress by inhibiting respiratory complex III [20]. Furthermore, it has been shown that the upregulation of NRF-1, mtTFA, and NF-κB was associated with increased levels of hydrogen peroxide in mtDNA-depleted HeLa cells [21].

It has been indicated that the redox status differs between normal and tumor cells. For example, levels of Mn superoxide dismutase, a mitochondrial antioxidant enzyme that scavenges superoxide anion radicals, were reduced in transformed cells compared to their normal counterparts [22]. Some tumors had higher levels of GSH in tumor cells than in normal cells [23], or were less responsive to agents stimulating lipid peroxidation [24,25]. On the other hand, characteristics of mitochondria and energy metabolism were often altered in tumors, such as the change in respiratory functions and mitochondrial morphology [26]. It has been hypothesized that altered mitochondrial physiology, by affecting apoptosis and cell signaling through ROS, may play important roles in cellular transformation [17]. Therefore, responses of normal and tumor cells to oxidative stress induced by CPT may be different.

In this study, we compared the effect of CPT on cytotoxicity, apoptosis, lipid peroxidation, and mitochondrial 12S rRNA transcript levels in normal human WI38 cells and in SV40-transformed WI38 (VA13) cells. We show that CPT exerted different effects on levels of lipid peroxidation and mitochondrial 12S rRNA between WI38 and VA13 cells although CPT treatment resulted in greater growth-inhibitory effect and cell death in VA13 cells.

MATERIALS AND METHODS

Cell Culture

The embryonic human lung fibroblast WI38 cells (ATCC CCL 75) and their SV40-transformed subline VA13 cells (ATCC CCL 75.1) were obtained from Riken Cell Bank, Japan. The passage number of WI38 cells used in this study was 28–33. Both cells were maintained in minimum essential media (MEM) with Earl's salts supplemented with 10% defined fetal bovine serum (HyClone, UT). The use of WI38 and VA13 cells as counterparts to a cell model for comparing the difference between normal and tumor cells has been previously reported [27,28].

Cytotoxicity Assay

Cytotoxicity was evaluated by the growth inhibition. CPT was purchased from Bristol-Myers Squibb S.p.A. (Italy) in the form of 0.5 mg/mL solution (Plantinex). Cells grown in 96-well tissue culture plates were treated with various doses of CPT 48 h before confluence. At the end of treatment, cells were incubated with reagents from the CellTiter 96 Aqueous One Solution Cell Proliferation Assay Kit (Promega, WI). The absorbance of reduced tetrazolium compound catalyzed by dehydrogenases in viable cells was recorded at 490 nm. On the other hand, cell number in 6-well plates was also counted after 48-h CPT treatment at the dose of 6.7 μM (2 μg/mL) to verify results using the colorimetric kit.

Microscopic Assessment of Nuclear Chromatin Condensation and Fragmentation

Extent of apoptosis was quantified by the presence of nuclear chromatin and fragmentation by staining the nuclei of cells with Hoechst 33342 dye, using previously described methods [29,30]. Hoechst 33342 dye is a minor groove-binding dye that can easily enter cells during the early state of apoptosis [31]. Cells grown on glass-bottomed and poly-D-lysine coated 35-mm dishes (MatTek Corp., Ashland, MA) were fixed in 4% paraformaldehye in phosphate-buffered saline (PBS) for 30 min, washed with PBS, and then incubated with Hoechst 33342 dye (Molecular Probes, Eugene, OR) at the final concentration of 1 μg/mL for 30 min. Cells were washed twice with PBS and fluorescence of the dye was visualized by exciting the dye at 340 nm with an inverted microscope equipped with an UV epifluorescence filter (TE200, Nikon, Tokyo, Japan). Random fields were selected and 300–500 cells were

counted. Percentage of apoptotic cells was calculated for each dish.

Detection of Esterified F_2-isoprostanes

The extraction and purification of F_2-isoprostanes from samples was performed according to the method described by Morrow and Roberts [32]. All organic solvents were purchased from Merck (Darmstadt, Germany). Phospholipids in cells were extracted by homogenizing cells in ice-cold Folch solution (chloroform/methanol, 2:1 v/v) containing 0.005% butylated hydroxytoluene (BHT) and hydrolyzed with 15% KOH. The hydrolyzed free F_2-isoprostanes were purified by performing solid-phase extraction using C_{18} columns and silica columns from J.T. Baker (Phillipsburg, NJ) with a 24-channel vacuum manifold from J.T. Baker [33]. The nitrogen-dried eluate was resuspended in the enzyme immunoassay (EIA) buffer. 15-F_{2t}-IsoP was then analyzed by using an 8-isoprostane EIA kit from Cayman Chemical (Ann Arbor, MI). The standard curve and concentrations of unknown samples were plotted and calculated by using the 4-parameter fit in the softmax Pro software (Molecular Devices, Sunnyvale, CA). The level of 15-F_{2t}-IsoP was normalized by the cell number of each sample.

Detection of Intracellular HNE-Modified Proteins

This method has been previously described by Motoori et al. [30]. Cells grown on glass-bottomed dishes were fixed with 4% paraformaldehyde in PBS. Cell membranes were permeabilized by 95% ethanol plus 5% acetic acid. After being washed with PBS twice and then with PBS containing 0.1% bovine serum albumin (BSA) twice, cells were incubated with anti-HNE-modified protein monoclonal antibody (Japan Institute for the Control of Aging, Japan) at the concentration of 0.5 μg/mL for 60 min and finally incubated with AlexaFlour 488 goat anti-mouse IgG (H + L) secondary antibody (Molecular Probes) at the concentration of 10 μg/mL for 60 min. Fluorescent images were acquired and quantified using a CSU-10 confocal laser scanning unit (Yokogawa Electric Co., Tokyo, Japan) coupled to an LX90 inverted microscope (Olympus Optical Co.) and a C5810-1 color-chilled 3CCD camera (Hamamatsu Photonics K.K., Japan). The AlexaFlour 488 was excited at 488 nm and the emission was filtered using a 515-nm barrier filter. The intensity of the laser beam, the gain of the amplifier, and the exposure time were held at 500 μW, 18 dB, and 5 s respectively. The focus of the cells was adjusted to the middle of Z-axis before exposing the cells to laser and taking images. Therefore, each field taken was only exposed to the laser once. Several fields were scanned randomly. Fluorescent intensity per unit area of each field was quantified using IPLab Spectrum version 3.0 software (Scanalytics Inc., VA). Data were presented as the relative intensity calculated by dividing mean fluorescence intensity of each field with that of one data from the WI38 control group.

Nonradioactive Northern Blot Analysis

Total RNA was isolated by the StrataPrep Total RNA Miniprep Kit with DNase I treatment (Stratagene, La Jolla, CA). The concentration of RNA was determined by measuring the absorbance at 260 nm. The ratio of absorbance at 260 to that at 280 nm was at least 1.8. The level of mitochondrial 12S rRNA was detected by nonradioactive Northern blot analysis modified from the manufacturer's instruction (The DIG System User's Guide for Filter Hybridization, Roche, Mannheim, Germany). Fifteen micrograms of total RNA was electrophoresed in 1.5% agarose gel containing formaldehyde [34] and transferred to the GeneScreen Neutral Nylon membranes (NEN, Boston, MA) in 10× SSC (3 M sodium chloride and 300 mM sodium citrate, pH 7.0 for 20× SSC). Digoxigenin (DIG)-labeled probes for mitochondrial genes were generated by polymerase chain reaction (PCR) using total DNA isolated from WI38 cells as the template and the PCR DIG Probe Synthesis Kit (Roche). Primers for 12S rRNA were 5′CCCCATACCCCGAACCAACC3′ and 5′GGAGTGGGTTTGGGGCTAGG3′. DIG-labeled probes for β-actin were also generated by PCR but using cDNA as the template and the primers 5′AGAGATGGCCACGGCTGCTT3′ and 5′ATTTGCGGTGGACGATGGAGG3′. Membranes with RNA were placed in a UV cross-linker at 0.12 J/cm^2, prehybridized in hybridization solution (50% deionized formamide, 5× SSC, 0.1% *N*-lauroyl-sarcosine, 0.02% SDS, 2% blocking reagent from Roche) at 42°C for 1 h, and then hybridized with gel-purified probes in hybridization solution at 42°C overnight. The membranes were then washed twice in the first wash buffer (2× SSC and 0.1% SDS) at room temperature and in the second wash buffer (0.5× SSC and 0.1% SDS) at 68°C. The DIG on hybridized probes was detected by the DIG Luminescent Detection Kit (Roche) with alkaline phosphatase-conjugated anti-DIG antibody according to the manufacturer's instruction. Chemiluminescent bands were detected by exposing the membranes to the BioMax ML film (Kodak, Rochester, NY) and the density on the film was analyzed by the ChemiDoc system (Biorad, Hercules, CA) or directly photographed and analyzed by the ChemiDoc. Total RNA isolated from mtDNA-depleted

143B-TK$^-$ (143B-TK$^-$-ρ^0) cells, which were obtained from Dr. Douglas C. Wallace at Emory University [35], was used as a negative control in the Northern blot analysis.

Statistical Analysis

Data were analyzed by SAS Win 8.1 software (SAS Institute, Cary, NC). Two-way analysis of variance (ANOVA) was first used to examine the interaction between cell type (WI38 vs. VA13) and treatment (control vs. CPT), that is, to examine whether WI38 cells reacted to the treatment effect differently from the way VA13 cells reacted to the treatment effect. If interaction between cell type and treatment was significant, one-way ANOVA was further used to compare the difference among multiple groups. All data were presented as mean ± standard deviation (SD). Statistical significance was considered when $p < 0.05$.

RESULTS

Inhibition of Cell Growth and Induction of Apoptosis by CPT

To compare the effect of 48-h CPT treatment on the growth of WI38 and VA13 cells, cytotoxicity was first accessed by colorimetric method for a dose range (0.67–66.7 μM) of CPT, and the exact cell number remaining after CPT treatment was counted in both cells at the dose of 6.7 μM. As shown in Figure 1, there was significantly higher cytotoxicity in VA13 cells than in WI38 cells after 48-h CPT treatment in the range from 3.34 to 33.4 μM. The dose that inhibited 50% growth (IC_{50}) for WI38 and VA13 cells was approximately 51.3 and 5.7 μM of CPT, respectively. By counting the cell number directly, we confirmed that 6.7 μM (2 μg/mL) of CPT treatment resulted in greater reduction in cell growth in VA13 than WI38 cells, following 48-h treatment (Figure 2). There was 51 and 27% reduction in cell number by 48-h CPT treatment in WI38 and VA13 cells, respectively. To further evaluate the role of apoptosis in the reduction of cell number after CPT treatment, percentage of apoptotic cells following Hoechst 33342 staining were counted under a fluorescence microscope. Table 1 shows that CPT caused significant increase of apoptotic cells in both WI38 and VA13 cells and the effect was greater in VA13 cells.

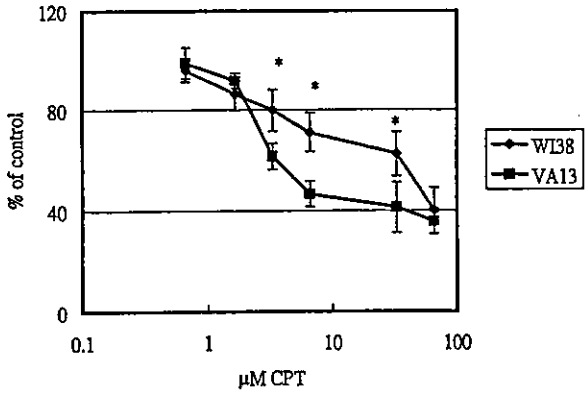

FIGURE 1. Cell proliferation assay for WI38 and VA13 cells treated with CPT for 48 h. Data were represented as percentage relative to mean of the control group ($n = 5$ for each group). The X-axis is in log scale.

Levels of Lipid Peroxidation

To compare lipid peroxidation after CPT treatment, cells were treated with CPT for 48 h at the dose of 6.7 μM and lipid peroxidation levels were measured. Figure 3 shows that levels of esterified 15-F_{2t}-IsoP were significantly increased in WI38 cells after CPT treatment, but not in VA13 cells. Furthermore, HNE-protein adducts were detected using immunofluorescent staining and the image is shown in Figure 4. Quantification of the fluorescent images indicated that intracellular levels of HNE were also elevated in WI38 cells, but not in VA13 cells (Table 2). These findings provided strong evidence for the occurrence of lipid peroxidation in WI38 cells

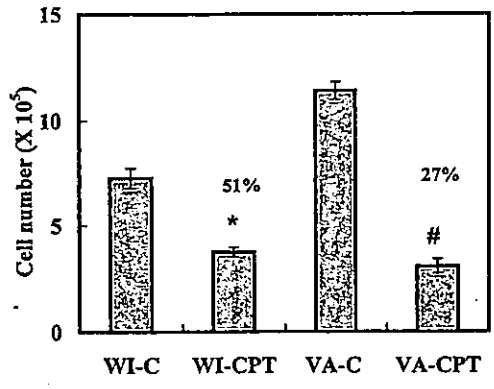

FIGURE 2. Cell count after 48-h CPT treatment. WI-C, control group of WI38 cells; WI-CPT, CPT (6.7 μM)-treated WI38 cells; VA-C, control group of VA13 cells; VA-CPT, CPT-treated VA13 cells. Two-way ANOVA was made ($n = 4$ for each group). Interaction between cell type and treatment was statistically significant ($p < 0.001$), indicating the reduction of cell number following CPT treatment was significantly different between WI38 cells (51% remained) and VA13 cells (27% remained). One-way ANOVA was further made and showed that CPT treatment resulted in significant inhibition of cell growth in either WI38 or VA13 cells. *, WI-CPT vs. WI-C ($p < 0.001$); #, VA-CPT vs. VA-C ($p = 0.03$).

TABLE 1. Microscopic Assessment of DNA Chromatin Condensation and Fragmentation by Hoechst 33342 Staining

Group	*Percentage of Apoptotic Cells*
WI38-control	0.616 ± 0.199
WI38-CPT	2.415 ± 0.702[a]
VA13-control	0.857 ± 0.458
VA13-CPT	5.053 ± 1.816[b]

Percentage of apoptotic cells were calculated from 300 to 500 cells counted. Data were obtained from four dishes for each group. Two-way ANOVA indicated significant interaction effect between cell type and treatment ($p = 0.03$). One-way ANOVA indicated that there was significant increase of percentage of apoptotic cells in either WI38 or VA13 cells.
[a]WI38-CPT vs. WI38-control ($p < 0.001$).
[b]VA13-CPT vs. VA13-control ($p = 0.003$).

as the results of F_2-isoprostanes and HNE agreed with each other.

Levels of 12S rRNA Relative to Nuclear β-actin mRNA

Since CPT can cause mitochondrial dysfunction [4] and mtDNA damage [36], we next determined the pattern of mitochondrial gene expression, which could be modulated by oxidative stress or mitochondrial dysfunction. We established nonradioactive Northern blot analysis using PCR-generated and DIG-labeled probes to detect steady-state RNA levels. Figure 5A shows the excellent quality of total RNA of each sample following electrophoresis. Figure 5B shows levels of mitochondrial 12S rRNA and β-actin mRNA from nucleus. After normalization to the density of β-actin bands in arbitrary densitometric units, levels of 12S rRNA gene were increased by 203 ± 52% and 132.5 ± 3%, relative to the control group, in WI38 and VA13 cells respectively, following CPT treatment from three sets of experiments, but the increase in WI38 was more.

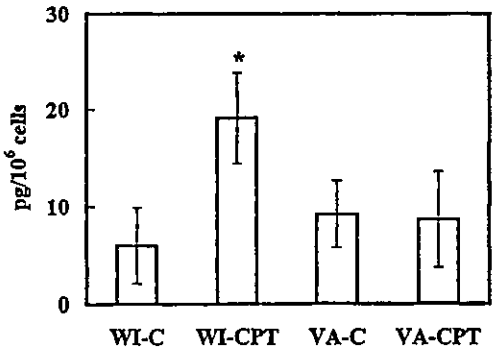

FIGURE 3. Levels of esterified 15-F_{2t}-IsoP in WI38 and VA13 cells. Cells were treated with 6.7 μM of CPT for 48 h. Data were represented as mean ± SD (n = 5–6 for each group). *, CPT-treated WI38 cells had significantly higher level of esterified 15-F_{2t}-IsoP than its control cells ($p = 0.001$). WI-C, WI-CPT, VA-C, and VA-CPT represent the same groups described in Figure 2.

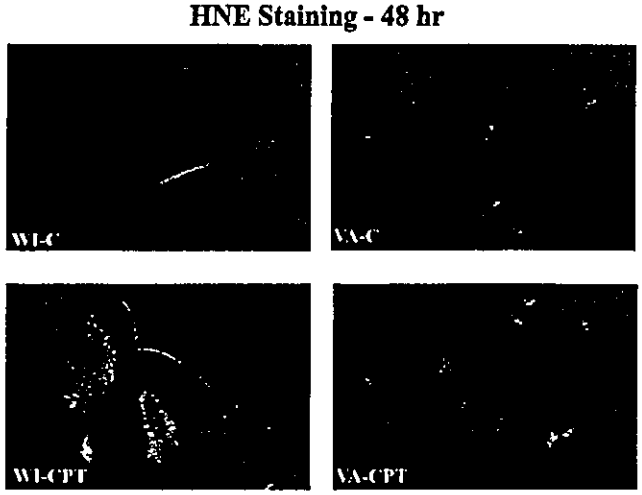

FIGURE 4. Immunofluorescent staining for detecting intracellular levels of HNE-protein adducts in cells. WI-C, WI-CPT, VA-C, and VA-CPT represent the same groups described in Figure 2.

DISCUSSION

We have shown that in spite of inducing greater growth inhibition and apoptosis in VA13 cells than in WI38 cells, CPT increased lipid peroxidation in WI38 cells but not in VA13 cells, indicating a differential response in transformed phenotypes. The results indicate that although CPT, as an anticancer drug, unsurprisingly has more greater inhibitory effect on the growth of VA13 cells, which have faster proliferation rate, it can preferentially cause oxidative damage to normal WI38 cells by inducing lipid peroxidation. We have also demonstrated that CPT could have a positive effect on transcription of mtDNA, and the increase of 12S rRNA in WI38 cells was greater than that in VA13 cells.

Because much lower doses of CPT and a longer treatment time were used in the current study, the results would be different from that of experiments using much higher acute doses [4,6]. There was no appreciable amount of lactate dehydrogenase released in the medium following the CPT treatment (data not shown). Although CPT also significantly increased the amount

TABLE 2. Quantification of Intracellular HNE Levels

Group	*Relative HNE Levels*
WI38-control	1.00 ± 0.05
WI38-CPT	1.23 ± 0.11[a]
VA13-control	1.08 ± 0.11
VA13-CPT	1.11 ± 0.08

Data were presented the ratio of relative fluorescence intensity to one WI38 control data. There were 13–15 data from three dishes for each group. The intracellular levels of HNE-protein adducts were significantly increased by CPT in WI38 cells but not in VA13 cells.
[a]WI38-CPT vs. WI38-control group ($p < 0.001$).

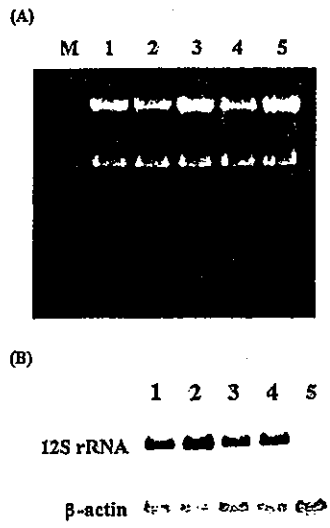

FIGURE 5. Northern blot analysis for the detection of mitochondrial 12S rRNA transcript level. RNA gel electrophoresis showed excellent quality of total RNA (A). Steady-state levels of mitochondrial 12S rRNA and nuclear β-actin mRNA in WI38 and VA13 cells before and after 48-h CPT treatment were shown (B). M, 0.16–1.77 Kb RNA ladder from GIBCO; 1, WI38 control; 2, CPT-treated WI38; 3, VA13 control; 4, CPT-treated VA13; 5, 143-B-TK$^-$-ρ^0 cells.

of apoptotic cells, there was only about 2.4 and 5.1% of apoptotic cells in CPT-treated WI38 and VA13 cells, respectively (Table 1). The results indicate that such small degree of apoptosis may contribute to greater cytotoxicity in VA13 cells but its significance was uncertain since degree of growth inhibition was much higher (Figure 2). Although it is known that oxidative stress is important in apoptosis [37], the results suggest that apoptosis induced by CPT in VA13 cells may not be associated with lipid peroxidation.

Detection of lipid peroxidation provides one reliable indicator for the occurrence of oxidative damage to cells. Most studies showing CPT-mediated lipid peroxidation applied a less specific indicator of lipid peroxidation, malondialdehyde [3]. In our study, we used two more specific markers of lipid peroxidation. There was one report showing that CPT treatment increased F_2-isoprostanes in normal renal tubular cells [6]. By using a much lower dose, we also showed an increase in F_2-isoprostanes levels in normal WI38 cells. In addition to F_2-isoprostanes, elevation of intracellular cytotoxic HNE was also found in WI38 cells following CPT treatment, which was first demonstrated in CPT toxicity by our study. We also first demonstrated preferential increase in lipid peroxidation levels by CPT in normal WI38 cells but not their transformed counterpart cells. It has been shown that HNE could not only activate NF-κB and induce apoptosis, but also further induce the formation of 15-F_{2t}-IsoP in normal cells [38]. There were many possible explanations as to how CPT caused lipid peroxidation in WI38 but not in VA13 cells. First, if GSH depletion was the major cause of lipid peroxidation, VA13 cells could have more protection because of higher total glutathione levels [27]. Increased formation of HNE in WI38 cells could further augment GSH depletion. However, as with the action of many anticancer drugs, CPT-mediated DNA damage by forming interstrand cross-links with DNA [39] may have a more detrimental effect on the growth of VA13 cells because of more active proliferating ability of VA13 cells. Second, if lipid peroxidation was initiated from mitochondria, the difference in the outcome of oxidative stress between WI38 and VA13 cells could be due to possible altered mitochondrial properties in VA13 cells, which requires further examination. Finally, there could be an altered lipid composition, such as the proportion of arachidonic acids, or altered metabolism and regulation of fatty acids in VA13 cells. As reviewed by Dianzani [24], normal liver and hepatoma cells generally have different levels and compositions of PUFAs. AH-130 Yoshida ascites tumors were much less responsive to stimulation that induced lipid peroxidation than were normal hepatocytes, but enrichment of arachidonic acids resulted in the restoration of the lipid peroxidation responses in hepatoma cells.

We have also demonstrated that CPT can augment steady-state levels of mitochondrial 12S rRNA. Since the formation of individual mitochondrial transcripts is generated from the same initial polycistronic transcript, which is controlled by mtTFA from the nucleus [15,40], only 12S rRNA transcript levels were examined. It has been shown that the upstream region of mtTFA gene has recognition sites for NRF-1, NRF-2, and Sp1 [41], which could be regulated by redox signaling [17]. It is possible that CPT can damage mtDNA via oxidative damage or by direct cross-linking [35,38]. It has been demonstrated that there was increased expression of both mitochondrial and nuclear genes associated with oxidative phosphorylation in tissues of patients carrying genetic mtDNA mutations [42]. Therefore, CPT may increase mitochondrial transcription by altering activities of nuclear-encoded transcription factors in response to oxidative stress, metabolic signals, or mtDNA damage. Furthermore, because HNE detected was bound to proteins and HNE may modulate the activity of redox-sensitive transcription factors [13,38], it is also possible that HNE can affect factors regulating mitochondrial gene expression. Higher lipid peroxidation levels in WI38 cells may contribute to the higher degree of 12S rRNA increase in WI38 cells than in VA13 cells. Possible different mitochondrial properties or regulatory mechanisms of mitochondrial genes between WI38 and VA13 cells may also contribute to this difference.

In conclusion, we have shown that CPT significantly increased levels of lipid peroxidation in WI38 cells, but not in VA13 cells. Our results suggest that CPT may preferentially induce lipid peroxidation in normal cells independent of the extent of growth inhibition and apoptosis or lipid peroxidation is less inducible by CPT in tumor cells. Nevertheless, the increase of lipid peroxidation would have toxic effects on normal cells by interfering normal membrane functions on cell membrane or intracellular organelles, such as mitochondria. Moreover, the higher increase of mitochondrial transcripts by CPT in WI38 cells may be associated with higher levels of lipid peroxidation in WI38 cells. These findings may have implications in managing CPT-induced toxicity by understanding the differential responses between normal and transformed cells to CPT.

ACKNOWLEDGMENT

We thank Ms. Chizuru Yamaguchi and Dr. Shizuko Kakinuma for helpful technical assistance.

REFERENCES

1. Cvitkovic E. Cumulative toxicities from cisplatin therapy and current cytoprotective measures. Cancer Treatment Rev 1998;24:265–281.
2. Hacker M. Toxicity of platinum-based anticancer drugs. In: Powis G, Hacker HP, editors. The Toxicity of Anticancer Drugs. New York: Pergamon Press; 1991. pp 82–105.
3. Kharbangar A, Khynriam D, Prasad SB. Effect of cisplatin on mitochondrial protein, glutathione, and succinate dehydrogenase in Dalton lymphoma-bearing mice. Cell Biol Toxicol 2000;16:3636–373.
4. Kruidering M, van de Water B, de Heer E, Mulder GJ, Nagelkerke JF. Cisplatin-induced nephrotoxicity in porcine proximal tubular cells: Mitochondria dysfunction of complex I to IV of the respiratory chain. J Pharmacol Exp Ther 1997;280:638–649.
5. Richter C, Gogvadze V, Laffranchi R, Schlabach R, Schweizer M, Suter M, Walter P, Yaffee M. Oxidants in mitochondria: From physiology to diseases. Biochim Biophys Acta 1995;1271:67–74.
6. Salahudeen A, Poovala V, Parry W, Pande R, Kanji V, Ansari N, Morrow J, Roberts J II. Cisplatin induced *N*-acetyl cysteine suppressible F_2-isoprostane production and injury in renal tubular epithelial cells. J Am Soc Nephrol 1998;9;1448–1455.
7. Rybak LP, Husain K, Whitworth C, Somani SM. Dose dependent protection by lipoic acid against cisplatin-induced ototoxicity in rats: antioxidant defense system. Toxicol Sci, 1999;47:195–202.
8. Morrow JD, Hill KE, Burk RF, Nammour RM, Badr KF, Roberts LJ II. A series of prostaglandin F_2-like compounds are produced in vivo in humans by a non-cyclooxygenase, free radical-catalyzed mechanism. Proc Natl Acad Sci USA 1990;87:9383–9387.
9. Morrow JD, Awad JA, Boss HJ, Blair IA, Roberts LJ II. Non-cyclooxygenase-derived prostanoids (F_2-isoprostanes) are formed in situ on phospholipids. Proc Natl Acad Sci USA 1992;89:10721–10725.
10. Roberts LJ II, Morrow JD. Measurement of F_2-isoprostanes as an index of oxidative stress in vivo. Free Radic Biol Med 2000;28:505–513.
11. Halliwell B, Gutteridge JMC. Free Radicals in Biology and Medicine, 3rd edition. New York: Oxford University Press; 1999. 936 p.
12. Esterbauer H, Schaur RJ, Zollner H. Chemistry and biochemistry of 4-hydroxynonenal, malonaldehyde and related aldehydes. Free Radic Biol Med 1991;11:81–128.
13. Leonarduzzi G, Arran MC, Basaga H, Chiarpotto E, Sevanian A, Poli G. Lipid oxidation products in cell signaling. Free Radic Biol Med 2000;28:1370–1378.
14. Wallace DC. Mitochondrial diseases in man and mouse. Science 1999;283:1482–1488.
15. Moraes C. What regulates mitochondrial DNA copy number in animal cell? Trends Genet 2001;17:199–205.
16. Poyton RO. Crosstalk between nuclear and mitochondrial genomes. Annu Rev Biochem 1996;65:563–607.
17. Preston TJ, Abadi A, Wilson L, Singh G. Mitochondrial contributions to cancer cell physiology: Potential for drug development. Adv Drug Delivery Rev 2001;49:45–61.
18. Esposito LA, Melov S, Panov A, Cotrell BA, Wallace DC. Mitochondrial disease in mouse results in increased oxidative stress. Proc Natl Acad Sci USA 1999;96:4820–4825.
19. Murdock DG, Boone BE, Esposito LA, Wallace DC. Up-regulation of nuclear and mitochondrial genes in the skeletal muscle of mice lacking the heart/muscle isoform of the adenine nucleotide translocator. J Biol Chem 1999;274:14429–14433.
20. Suzuki H, Kumagai T, Goto A, Sugiura T. Increase in intracellular hydrogen peroxide and upregulation of a nuclear respiratory gene evoked by impairment of mitochondrial electron transfer in human cells. Biochem Biophys Res Commun 1998;249:542–545.
21. Miranda S, Foncea R, Guerrero J, Leighton JF. Oxidative stress and upregulation of mitochondrial biogenesis genes in mitochondrial DNA-depleted HeLa cells. Biochem Biophys Res Commun 1999;258:44–49.
22. Oberley LW, Buettner GR. Role of superoxide dismutase in cancer. Cancer Res 1979;39:1141–1149.
23. Russo A, DeGraff W, Friedman N, Mitchell JB. Selective modulation of glutathione levels in human normal versus tumor cells and subsequent differential response to chemotherapy drugs. Cancer Res 1986;46:2845–2848.
24. Dianzani MU. Lipid peroxidation and cancer: A critical reconsideration. Tumori 1989;75:351–357.
25. Jones GRN. Cancer destruction in vivo through disrupted energy metabolism part II. Lipid peroxidation and cell death; drug resistance as a consequence of reversible cellular injury. Physiol Chem Phys & Med NMR 1992;24:181–194.
26. Pederson PL. Tumor mitochondria and the biogenetics of cancer cells. Prog Exp Tumor Res 1978;22:190–274.
27. Wan XS, Clair DK. Differential cytotoxicity of buthionine sulfoximine to "normal" and transformed human lung fibroblast cells. Cancer Chemother Pharmacol 1993;33:210–214.
28. Chen ZP, Schell JB, Ho C-T, Chen KY. Green tea epigallocatechin gallate shows a pronounced growth inhibitory effect on cancerous cells but not on their normal counterparts. Cancer Lett 1998;129:173–179.

29. Majima HJ, Oberley TD, Furukawa K, Mattson MP, Yen H-C, Szweda LI, St. Clair DK. Prevention of mitochondrial injury by manganese superoxide dismutase reveals a primary mechanism for alkaline-induced cell death. J Biol Chem 1998;273:8217–8224.
30. Motoori S, Majima HJ, Ebara M, Kato H, Hirai F, Kakinuma S, Yamaguchi C, Ozawa T, Nagano T, Tsujii H, Saisho H. Overexpression of mitochondrial manganese superoxide dismutase protects against radiation-induced cell death in the human hepatocellular carcinoma cell line HLE. Cancer Res 2001;61:5382–5388.
31. Haugland RP. Handbook of Fluorescent Probes and Research Products, Web edition (www.probes.com/handbook). Eugene, OR: Molecular Probes, Inc; 2002.
32. Morrow JD, Roberts LJ II. F_2-isoprostanes: Prostaglandin-like products of lipid peroxidation. In: Punchard NA, Kelly FJ, editors. Free Radicals. A Practical Approach. New York: Oxford University Press; 1996. pp 147–157.
33. Yen H-C, Cheng H-S, Hsu Y-T, Ho H-J, Nien C-Y, Lee Y-S. Effects of age and health status on levels of urinary 15-F_{2t}-isoprostane. J Biomed Lab Sci 2001;13:24–28.
34. Sambrook J, Russell DW. Molecular Cloning. A Laboratory Manual, 3rd edition. Cold Spring Harbor, New York: Cold Spring Harbor Laboratory Press; 2001.
35. Trounce I, Schmiedel J, Yen H-C, Hosseini S, Brown MD, Olson JJ, Wallace DC. Cloning of neuronal mtDNA variants in cultured cells by synaptosome fusion with mtDNA-less cells. Nucleic Acids Res 2000;28:2164–2170.
36. Olivero OA, Chang PK, Lopez-Larraza DM, Semino-Mora MC, Poirier MC. Preferential formation and decreased removal of cisplatin-DNA adducts in Chinese hamster ovary cell mitochondrial DNA compared to nuclear DNA. Mutat Res 1997;391:79–86.
37. Chandra J, Samali A, Orrenius S. Triggering and modulation of apoptosis by oxidative stress. Free Radic Biol Med 2000;29:323–333.
38. Ruef J, Moser M, Bode C, Kubler W, Runge MS. 4-Hydroxylnonenal induced apoptosis, NF-κB-activation and formation of 8-isoprostane in vascular smooth muscle cells. Basic Res Cardiol 2001;96:143–150.
39. Zou Y, van Houten B, Farrell N. Sequence specificity of DNA–DNA interstrand cross-link formation by cisplatin and dinuclear platinum complexes. Biochemistry 1994;33:5405–5410.
40. Attardi G. Biogenesis of mitochondria. Ann Rev Cell Biol 1988;4:289–333.
41. Virbasius JV, Scarpulla RC. Activation of human mitochondrial transcription factor A gene by nuclear respiratory factors: A potential link between nuclear and mitochondrial gene expression in organelle biogenesis. Proc Natl Acad Sci USA 1994;92:1309–1313.
42. Heddi A, Stepien G, Benke PJ, Wallace DC. Coordinate induction of energy gene expression in tissues of mitochondrial disease patients. J Biol Chem 1999;274:22968–22976.

研究成果の刊行物・別刷
平成16年度

ELSEVIER

Brain & Development 26 (2004) 480

BRAIN & DEVELOPMENT
Official Journal of the Japanese Society of Child Neurology

www.elsevier.com/locate/braindev

Discussion

MELAS and L-arginine therapy

Yasutoshi Koga*

Department of Pediatrics and Child Health, Kurume University School of Medicine, 67 Asahi-Machi, Kurume, Fukuoka 830-0011, Japan

Received 30 January 2004; received in revised form 22 February 2004; accepted 23 February 2004

Mitochondrial myopathy, encephalopathy, lactic acidosis and stroke-like episodes (MELAS) is a maternally inherited multisystem mitochondrial disorder characterized by stroke-like episodes before 20 years of age [1]. Mitochondrial angiopathy, with degenerative changes in small arteries and arterioles, has been reported in many MELAS patients [2]; these blood vessels have been designated as strongly succinate dehydrogenase-reactive vessels (SSVs) [3]. However, the primary cause for stroke-like episodes in young MELAS patients—whether mitochondrial cytopathy, angiopathy, or both—remains controversial. Many therapeutic trials have been undertaken to cure mitochondrial disorders, but not for the acute stroke phase of MELAS. Based on a hypothesis that stroke-like episodes in MELAS are caused by segmental impairment of vasodilation in intracerebral arteries, L-arginine has been used for therapeutic trials in MELAS patients during the acute phase of stroke. We found that L-arginine therapy quickly decreased severity of stroke-like symptoms in MELAS, enhanced dynamics of microcirculation, and also reduced tissue injury from ischemia [4]. L-arginine is a potent vasodilator via endothelial function through nitric oxide (NO) production [5]. Cardioprotective effects of L-arginine and NO are associated with endothelial cell preservation [6], decreased neutrophil activation [7], improved coronary blood flow, and reduced free radical-mediated injury [8]. Although the molecular mechanism of L-arginine therapy in MELAS is not known, it is a potential new therapy for use at the acute phase of stroke-like episodes in MELAS.

In this paper, Dr Kubota and colleagues have performed a therapeutic trial to a 16-year-old girl with an acute phase of MELAS, using L-arginine infusion in order to improve the symptoms from stroke-like episodes. Among one out of five severe stroke-like episodes, L-arginine was added on the conventional steroid and glycerol therapy at the fifth episode. The authors described that L-arginine improved the symptoms much earlier than those without L-arginine infusion and shortened the duration of hospitalization. They measured the lactate level by MRS, which is a good indicator of the therapeutic effect. This is a case report describing a successful therapeutic result in MELAS. The finding will provide information about a new therapeutic approach to this currently incurable disease.

References

[1] Pavlakis SG, Phillips PC, DiMauro S, Rowland LP. Mitochondrial myopathy, encephalopathy, lactic acidosis, and strokelike episodes: a distinctive clinical syndrome. Ann Neurol 1984;16:481–8.

[2] Ohama E, Ohara S, Ikuta F, Tanaka K, Nishizawa M, Miyatake T. Mitochondrial angiopathy in cerebral blood vessels of mitochondrial encephalomyopathy. Acta Neuropathol 1987;74:226–33.

[3] Hasegawa H, Matsuoka T, Goto Y, Nonaka I. Strongly succinate dehydrogenase-reactive blood vessels in muscles from patients with mitochondrial myopathy, encephalopathy, lactic acidosis and stroke-like episodes. Ann Neurol 1991;13:1439–45.

[4] Koga Y, Ishibashi M, Ueki I, Yatsuga S, Fukiyama R, Akita Y, Matsuishi T. Effects of L-arginine on the acute phase of strokes in three patients with MELAS. Neurology 2002;58:827–8.

[5] Wang XL, Sim AS, Badenhop RF, McCredie RM, Wilcken DE. A smoking-dependent risk of coronary artery disease associated with a polymorphism of the endothelial nitric oxide synthase gene. Nat Med 1996;2:41–5.

[6] Shiono N, Rao V, Weisel RD, Kawasaki M, Li RK, Mickle DA, et al. L-Arginine protects human heart cells from low-volume anoxia and reoxygenation. Am J Physiol Heart Circ Physiol 2002;282:805–15.

[7] Kubes P, Suzuki M, Granger DN. Nitric oxide: an endogeneous modulator of leukocyte adhesion. Proc Natl Acad Sci USA 1991;88:4651–5.

[8] Radomski MW, Moncada S. The biological and pharmacological role of nitric oxide in platelet function. Adv Exp Med Biol 1993;344:251–64.

* Tel.: +81-942-31-7565; fax: +81-942-38-1792.
E-mail address: yasukoga@med.kurume-u.ac.jp (Y. Koga).

doi:10.1016/j.braindev.2004.02.007

ELSEVIER

Noonan Syndrome, Moyamoya-like Vascular Changes, and Antiphospholipid Syndrome

Yushiro Yamashita, MD,
Akira Kusaga, MD,
Yasutoshi Koga, MD,
Shin-ichiro Nagamitsu, MD, and
Toyojiro Matsuishi, MD

This reports describes a 12-year-old Japanese female with Noonan syndrome who had antiphospholipid syndrome and moyamoya-like vascular changes. She presented choreic movements in her face and extremities. She manifested phenotypic features of Noonan syndrome with short stature, mental retardation, and a webbed neck. Magnetic resonance angiography revealed occlusion of bilateral internal carotid arteries and moyamoya-like vascular changes around the basal ganglion region. Pimozide completely resolved the patient's choreic movements. Tests for anticardiolipin antibody and lupus anticoagulant were positive. The patient has manifested no symptoms for 2 years with pimozide, aspirin, and growth hormone treatment, without further aggravation of moyamoya-like vascular changes. This article is the first report of Noonan syndrome with antiphospholipid syndrome and moyamoya-like vascular lesions.

Yamashita Y, Kusaga A, Koga Y, Nagamitsu S, Matsuishi T. Noonan syndrome, moyamoya-like vascular changes, and antiphospholipid syndrome. Pediatr Neurol 2004;31: 364-366.

Introduction

Noonan syndrome is characterized by a normal karyotype and clinical features that resemble Turner syndrome. An association between Noonan syndrome and moyamoya has been reported in only two cases [1,2]. In adults, the association between strokes and antiphospholipid antibodies has been established, but such an association with moyamoya disease has not been identified.

This report describes for the first time a first patient with a rare combination of Noonan syndrome, moyamoya-like vascular changes, and antiphospholipid syndrome.

Case Report

In June 2001, a 12-year-old female experienced difficulty in walking because of involuntary movement in the left upper and lower limbs. She was observed at Saga University Hospital. Cranial magnetic resonance imaging was normal. By the end of June, her symptoms improved. She was diagnosed as having antiphospholipid syndrome because of thrombocytopenia and positive anticardiolipin antibody. None of her family members had similar problems. The family did not return to the hospital because the patient was completely well. In February 2002, however, she had chorea again starting from the right hand and extending to the right foot. In April, her chorea extended to the left side and she began to speak less. The family saw a neurosurgeon, and cranial magnetic resonance angiography revealed moyamoya-like vascular changes. The patient was then referred to Kurume University Hospital for further evaluation and treatment.

On admission, her height was 120.8 cm (−5 SD) and her weight was 27 kg (−2 SD). She had multiple purpura lesions in her extremities. She manifested phenotypic features of Noonan syndrome, including a webbed and short neck, low posterior hair lines, low-set and abnormal auricles, and hyperterolism. She manifested no signs of lupus or secondary sexual development. The patient had no history of seizures, and no cardiac lesions were evident. There was no family history of thrombosis.

Neurologically, she was alert, but had dysarthria caused by facial chorea. Her chorea was more prominent in the right side upper and lower limbs with hypotonia. Her deep tendon reflexes were elevated, and the Babinski reflex was positive on the right side. Her full intelligence quotient (Wechsler Intelligence Scale for Children–third version [WISC-III]) was 53; verbal intelligence quotient 60, performance intelligence quotient 55. Her social performance was relatively good, and she was in a mainstream classroom.

Complete blood count revealed low platelets (90,000). Prothrombin time and activated partial thromboplastin time were mildly prolonged, and lupus anticoagulant 1.76 (normal <1.3), anticardiolipin antibody 100 (normal <10), anti-b2 glycoprotein, and antinuclear antibody were positive. Anti-Sm, anti-RNA, anti-SS-A/Ro, and anti-SS-B/La antibodies were negative. Protein C and S were normal. Her bone age was delayed, and growth hormone secretion was abnormal by both an L-arginine and glucagon loading test. Auditory brainstem response and electroencephalogram were normal. The cranial computed tomography revealed mild

From the Department of Pediatics and Child Health, Kurume University School of Medicine, Kurume, Japan.

Communications should be addressed to:
Dr. Yamasihta; Department of Pediatics and Child Health;
Kurume University School of Medicine; 67 Asahi-machi;
Kurume 830-0011, Japan.
Received February 2, 2004; accepted May 3, 2004.

doi:10.1016/j.pediatrneurol.2004.05.015 • 0887-8994/04/$—see front matter

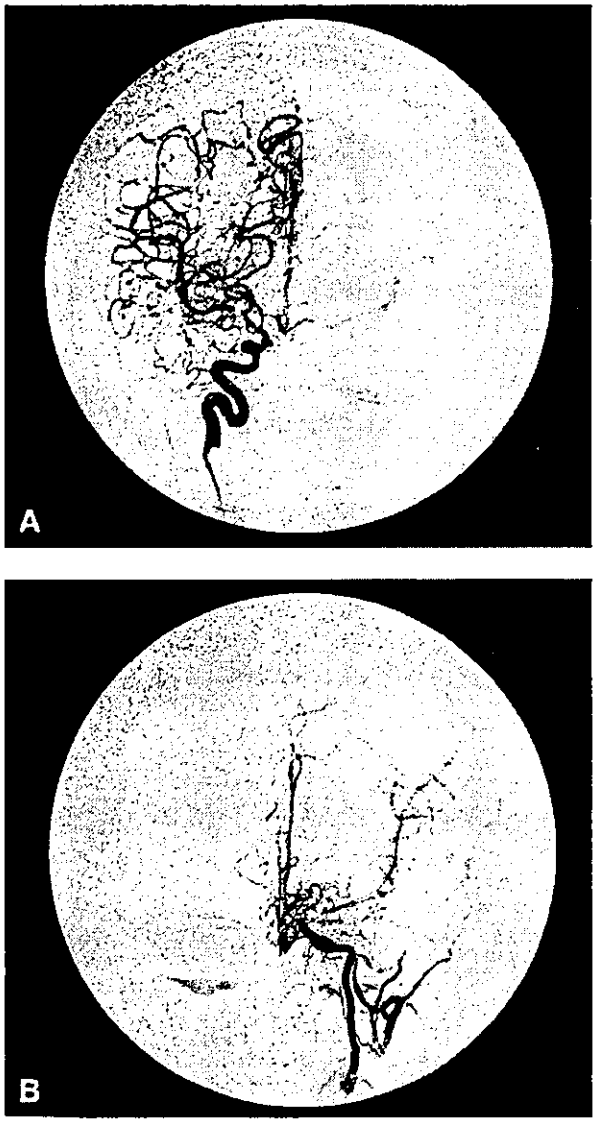

Figure 1. Cerebral angiogram: Right carotid angiogram indicated severe stenosis of internal carotid artery terminal lesion (A), and left carotid angiogram (B) demonstrated severe stenosis in the supraclinoid segment and collateral moyamoya-like vascular changes distal to the stenosis. The left internal carotid artery was narrower than the left side.

atrophy of the parietal lobe in the right hemisphere. The cranial magnetic resonance imaging revealed low-intensity areas in the basal ganglia on the right side. The cranial magnetic resonance angiography documented bilateral stenosis of the internal carotid arteries, which was more prominent on the right side, and moyamoya-like vascular changes in the bilateral basal ganglia and thalami region (Fig 1). Her chromosome count was normal (46 XX).

The patient was treated with a D2 antagonist, pimozide (1.5 mg/day), and her chorea completely resolved by the end of May. She has manifested no symptoms for 2 years with pimozide, aspirin (100 mg/day), and growth hormone treatment, with no further aggravation of moyamoya-like vascular changes.

Discussion

This patient was diagnosed with antiphospholipid syndrome because she had thrombocytopenia, positive anticardiolipin antibody, and lupus anticoagulant. These findings were repeatedly demonstrated at 10-month intervals. Furthermore, the patient manifested characteristic features of Noonan syndrome, including short stature, facial and neck abnormalities, mild mental retardation, and a normal karyotype. On magnetic resonance angiography, she also manifested moyamoya-like vascular changes in bilateral carotid arteries and basal ganglia. She was diagnosed with moyamoya disease because she had underlying Noonan syndrome and antiphospholipid syndrome.

Booth et al. have reported a 7-year-old female with an ischemic event in association with repeated elevation of anticardiolipin antibody [3]. They demonstrated bilateral moyamoya-like vascular changes. The patient was treated with warfarin for 5 months, followed by aspirin. Eleven months after the treatment, a marked improvement in blood flow with decreased stenosis of the left internal carotid was observed. They speculated that the development of moyamoya-like vascular changes might be secondary to initial thrombosis and stenosis of the basal cerebral vasculature with subsequent formation of collateral vessels. Takahashi et al. reported eight children with acute hemiplegia, with three being diagnosed as having infarctions due to moyamoya [4]. Anticardiolipin immunoglobulin G antibody was positive in three of the five with idiopathic infarction, but none with moyamoya disease, suggesting that the etiology of the infarct might be distinct from that in the patients with idiopathic infarction. In contrast, Bonduel et al. reported detecting prothrombotic disorders in 4 of 10 patients with moyamoya disease, suggesting its role in the pathogenesis of moyamoya [5]. Shoning et al. reported eight children who suffered from cerebrovascular ischemia or stroke in which antiphospholipid antibodies were detected. In two patients, stenoses of the basal cerebral arteries were present; a 5-year-old female with moyamoya-like vascular changes manifested improved circulation after treatment with aspirin and intravenous immunoglobulin, whereas a male patient required surgery for encephalo-duro-arterio-synangiosis [6].

There have been only two case reports of Noonan syndrome and moyamoya [1,2]. One of these patients had activated protein C resistance, which was thought to be coincidental. Antiphospholipid antibodies were not measured in these cases. Both patients were treated with aspirin and were responsive to nonsurgical therapy.

Encephalo-duro-arterio-synangiosis surgery was also considered for the patient in the present report; we decided not to pursue this route, however, because pimozide dramatically improved her symptoms and no further recurrence or progression of moyamoya-like vascular change occurred. In patients with moyamoya disease or moyamoya-like vascular changes, the possibility of antiphospholipid syndrome should be considered.

The authors gratefully acknowledge the assistance of Dr. Muneyuki Matsuo at the University of Saga, Department of Pediatrics.

References

[1] Ganesan V, Kirkham FJ. Noonan syndrome and moyamoya. Pediatr Neurol 1997;16:256-8.

[2] Tang KT, Yang W, Wong J, Lee KY. Noonan syndrome associated with moyamoya disease: Report of one case. Acta Peditr Tw 1999;40:274-6.

[3] Booth F, Yanofsky R, Ross IB, Lawrence P. Primary antiphospholipid syndrome with moyamoya-like vascular changes. Pediatr Neurosurg 1999;31:45-8.

[4] Takahashi J, Sugita K, Miyazato S, Sakao E, Miyamoto H, Niimi H. Antiphospholipid antibody syndrome in childhood strokes. Pediatr Neurol 1995;13:323-6.

[5] Bonduel M, Hepner M, Sciuccati G, Torres AF, Tenembaum S. Prothrombotic disorders in children with moyamoya syndrome. Stroke 2001;32:1786-92.

[6] Shöning M, Klein R, Krägeloh-Mann I, et al. Antiphospholipid antibodies in cerebrovascular ischemia and stroke in childhood. Neuropediatrics 1994;25:8-14.

HIGH LIGHT

L-Arginine improves the symptoms of strokelike episodes in MELAS

Abstract—Based on the hypothesis that mitochondrial myopathy, encephalopathy, lactic acidosis, and strokelike episodes (MELAS) are caused by impaired vasodilation in an intracerebral artery, the authors evaluated the effects of administering L-arginine, a nitric oxide precursor. Patients were administered L-arginine intravenously at the acute phase or orally at the interictal phase. L-Arginine infusions significantly improved all strokelike symptoms, suggesting that oral administration within 30 minutes of a stroke significantly decreased frequency and severity of strokelike episodes.

NEUROLOGY 2005;64:710–712

Y. Koga, MD, PhD; Y. Akita, MD, PhD; J. Nishioka, MD; S. Yatsuga, MD; N. Povalko, MD; Y. Tanabe, MD, PhD; S. Fujimoto, MD, PhD; and Toyojiro Matsuishi, MD, PhD

Mitochondrial myopathy, encephalopathy, lactic acidosis, and strokelike episodes (MELAS) is a maternally inherited, multisystem mitochondrial disorder.[1] The primary cause of strokelike episodes in young patients with MELAS, whether mitochondrial cytopathy, angiopathy, or both, remains controversial. Based on the hypothesis that strokelike episodes in MELAS are caused by segmental impairment of vasodilation in intracerebral arteries, we administered L-arginine by IV administration during the acute phase of strokelike episodes and by oral administration during the interictal phase.

Methods. *Patients.* We studied 24 patients referred to the hospital with MELAS diagnosed according to clinical, muscle pathologic, and genetic studies and 72 healthy control subjects (table 1). Patients with congenital anomalies, sepsis, IV hyperalimentation, diabetes mellitus, cardiac failure, or a bedridden state were excluded from this study.

Study design. All patients or patients' parents gave written informed consent, and the L-arginine study protocol was approved (Kurume University IRB no. 9715). The study design was chosen because of patients' availability and finances did not permit a balanced, randomized design involving multiple centers. Our strokelike episodes fulfilled the criteria that patients have migraine headache, vomiting, convulsion, and transient blindness with brain image suggesting focal brain abnormality. Twenty-four patients with a total of 34 strokelike episodes took part in this study of L-arginine versus placebo, following a previously described protocol.[2] The severity of a strokelike attack (convulsion, cortical blindness, hemiparesis, or abnormality in brain images associated with headache and vomiting) was similar when either L-arginine or placebo was administered.

Six patients were treated by oral administration of L-arginine to prevent strokelike episodes. Four to 24 g of L-arginine (Arugi U, Ajinomoto Pharma; 0.15 to 0.3 g/kg/d) were given orally for 18 months. Patients were monitored clinically and biochemically as described previously once every 2 weeks. When patients were admitted to the hospital with a strokelike episode, the following symptoms were scored: headache (present: 1, none: 0), vomiting (present: 1, none: 0), teichopsia (present: 1, none: 0), convulsion (present: 1, none: 0) and hemiparesis (present: 1, none; 0).[3] For each admission during the study period, these scores were summed as the severity score for the stroke. Frequency of admission was taken to be the frequency of strokelike episodes. Severity and frequency were related to time as number and month and were compared between periods 18 months before and after oral administration of L-arginine in the same patient.

Analysis of amino acids, asymmetric dimethylarginine (ADMA),[4] nitric oxide (NOx),[5] cyclic guanosine monophosphate (cGMP)[6] were measured using described methods.

Analysis. Plasma concentrations of amino acids, NOx, and ADMA in patients in the acute or interictal phase of MELAS were compared with those in controls using unpaired t tests, with Bonferroni corrections for outlying values. Concentrations of L-arginine, L-citrulline, NOx, ADMA, and cGMP in plasma obtained before, 30 minutes after, and 24 hours after L-arginine infusion were compared with those in controls using paired t tests. Statistical analysis of clinical improvement was performed using Fisher's exact test. Frequency and severity of strokelike episodes in six patients with MELAS after long-term oral L-arginine supplementation were compared with those in the same patients without supplementation using a nonparametric Mann–Whitney U test. All data are presented as means ± SD. p Values of 0.05 or less were considered to indicate significance.

Results. Baseline characteristics of the 24 patients and 72 controls are shown in table 1. Mean plasma concentrations of L-arginine and L-citrulline were lower in both acute (L-arginine: 47 ± 13 μmol/L; L-citrulline: 23 ± 10 μmol/L) ($p < 0.01$) and interictal phases (L-arginine: 84 ± 26 μmol/L; L-citrulline: 26 ± 10 μmol/L) ($p < 0.01$) of MELAS than in controls (L-arginine: 108 ± 28 μmol/L; L-citrulline: 35 ± 9 μmol/L). Concentrations of L-arginine in the acute phase were also significantly lower than in the interictal phase, whereas those of L-citrulline did not show a significant phase-related change. NOx concentrations were lower in the acute phase (24 ± 10 μmol/L) ($p < 0.01$) of MELAS than in controls (45 ± 30 μmol/L), whereas in the interictal phase (91 ± 44 μmol/L) ($p < 0.01$), they were higher than in controls. Conversely, concentrations of ADMA did not significantly differ between controls and acute phase, although the ADMA/L-arginine ratio was higher in the acute phase (0.011 ± 0.004) ($p < 0.01$) than in the controls (0.005 ± 0.001) or in the interictal phase (0.005 ± 0.001).

From the Department of Pediatrics and Child Health (Drs. Koga, Akita, Nishioka, Yatsuga, Povalko, and Matsuishi), Kurume University School of Medicine, Fukuoka, Japan; Department of Pediatric Neurology (Dr. Tanabe), Chiba Children's Hospital, Chiba, Japan; Department of Pediatrics (Dr. Fujimoto), Nagoya City University School of Medicine, Nagoya, Japan; and Research Centre for Medical Genetics RAMNS (Dr. Povalko), Moscow, Russia.

Supported in part by grants 13670853 and 16390308 from the Ministry of Culture and Education in Japan; H14-006, and H14-team(syouni)-005 from Evidence-based Medicine, Ministry of Health, Labor and Welfare in Japan; Uehara Memorial Foundation; and Morinaga Hoshikai.

Received June 18, 2004. Accepted in final form October 4, 2004.

Address correspondence and reprint requests to Dr. Yasutoshi Koga, Department of Pediatrics and Child Health, Kurume University School of Medicine, 67 Asahi-Machi, Kurume City, Fukuoka 830-0011, Japan; e-mail: yasukoga@med.kurume-u.ac.jp

Table 1 Baseline characteristics of the patients with MELAS and controls

Variable	Patients with MELAS (n = 24)	Controls (n = 72)
Age, y (range)	19.6 ± 12.5 (8.2–30.3)	21.5 ± 10.4 (4.3–35.4)
Gender, M/F	8/16	27/45
BMI	17.8 ± 3.6*	20.4 ± 2.3
Height	−2.2 ± 0.8*	0.2 ± 0.9
Alanine, μmol/L plasma	514 ± 164*	406 ± 121
Pyruvate, μmol/L	0.22 ± 0.06*	0.08 ± 0.05
Lactate, μmol/L	4.5 ± 1.8*	0.8 ± 0.2
L/P ratio	19.8 ± 2.9*	10.5 ± 1.8
Total cholesterol	139 ± 27	135 ± 38
LDL cholesterol	13.8 ± 3.7	14.6 ± 5.9
A3243G in muscle, %	68 ± 16	ND
Ragged-red fibers in muscle, %	3.6 ± 1.9	ND

Plus-minus values are means ± SD.
* $p < 0.05$ compared with controls.

MELAS = mitochondrial myopathy, encephalopathy, lactic acidosis, and strokelike episodes; BMI = body mass index; L/P = lactate pyruvate; LDL = low density lipoprotein; ND = not detectable.

Symptoms and biochemical measurements after L-arginine therapy in the acute phase of strokelike episodes in MELAS are shown in table 2 and the figure. After administration of L-arginine, all symptoms suggesting stroke dramatically improved. No adverse effects occurred, except headache, when L-arginine was infused too rapidly in two patients. With treatment, concentrations of lactate and pyruvate, L-arginine, L-citrulline, NOx, cGMP, and ADMA returned to interictal-phase concentrations within 24 hours.

After oral L-arginine supplementation, the frequency and severity of symptoms caused by the stroke had decreased dramatically. Frequency of strokelike episodes after treatment (0.09 ± 0.09) ($p < 0.05$) decreased compared with before supplementation (0.78 ± 0.42). The severity score after treatment (0.17 ± 0.18) ($p < 0.05$) was also lower than before supplementation (2.04 ± 0.34). After L-arginine supplementation, no patient with MELAS had a major strokelike attack, including hemiconvulsion or hemiparesis, but only headache or teichopsia. Plasma concentrations of L-arginine in patients with MELAS ranged from 82 to 120 μmol/L (mean ± SD 92 ± 17 μmol/L) after initiation of L-arginine supplementation.

Discussion. L-Arginine, which plays an important role in endothelium-dependent vascular relaxation, was significantly lower in both the acute and interictal phases of MELAS than in control subjects. Why plasma L-arginine is decreased in the acute phase of MELAS remains to be elucidated. We analyzed the

Table 2 Effects of L-arginine on the clinical symptoms in acute phase of MELAS

	Time after administration			
	Before	15 min	30 min	24 h
Headache (improvement of score from 3/2 to 1/0)				
L-Arginine	0/22	2/22	18/22*	21/22*
Placebo†	0/12	0/12	1/12	1/12
Clinical disability (improvement of score from 3/2 to 1/0)				
L-Arginine	0/22	3/22	16/22*	20/22*
Placebo†	0/12	0/12	1/12	1/12
Nausea				
L-Arginine	0/22	2/22	15/22*	22/22*
Placebo†	0/12	0/12	0/12	1/12
Vomiting				
L-Arginine	0/22	3/22	18/22*	22/22*
Placebo†	0/12	0/12	0/12	1/12
Hemi-blindness (transient)				
L-Arginine	0/7	2/7	4/7*	7/7*
Placebo†	0/4	0/4	1/4	1/4
Teichopsia				
L-Arginine	0/22	0/22	8/22*	19/22*
Placebo†	0/12	0/12	0/12	0/12

Numbers indicate the number of occasions when improvement was seen relative to the total number of episodes.
* $p < 0.05$ by Fisher's exact test.
† 5% dextrose (0.5 g/kg/dose) in eight episodes, and D-arginine in four episodes.

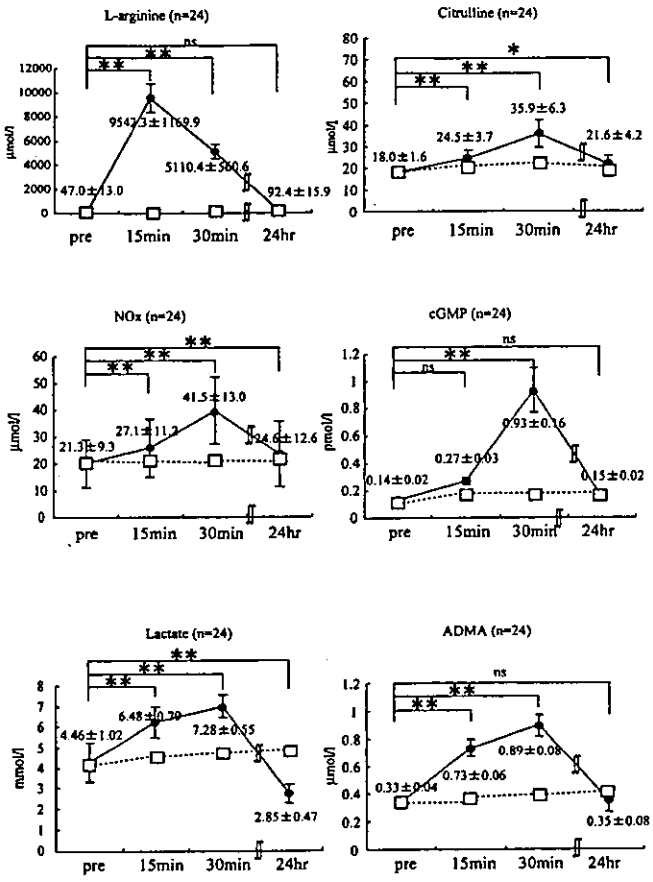

*Figure. Plasma concentrations of L-arginine, L-citrulline, nitric oxide (NOx), cyclic guanosine monophosphate (cGMP), lactate, and asymmetric dimethylarginine (ADMA) before and after L-arginine therapy in the acute phase of strokelike episodes in MELAS. Data represent mean ± SD (μmol/L) (n = 24). *p < 0.05; **p < 0.01 vs values before L-arginine therapy. ns = not significant. Filled circles show biochemical analysis after L-arginine therapy. Open squares show biochemical analysis after administration of placebo.*

correlation in all amino acids and found that the decrease of L-arginine in the acute phase is not influenced by urea cycle activities but may be caused by endothelial dysfunction (data not shown). A low L-arginine concentration and a relatively high ADMA concentration may predispose to strokelike episodes in MELAS. Impairment of endothelial function associated with relatively increased ADMA concentrations is reversed by IV L-arginine.[7] Consistent with these data, L-arginine infusion improved the ischemic process during the acute phase of MELAS.

Focal cerebral hyperemia has been reported in MELAS.[8] Although the underlying mechanisms are incompletely understood, hyperemia is thought to reflect vasodilation caused by local metabolic acidosis in the area of the infarct or by the foci of periodic epileptiform discharge.[9] Because the above studies were performed several days or several weeks after the onset of a strokelike episode, secondarily induced NOx production generated by inducible NOx synthase in the injured region may alter evidence of the primary pathophysiologic abnormality. In an analysis of SPECT findings in young patients with MELAS at a very early stage of strokelike episodes (within 3 hours after onset), we found hypoperfusion in the region affected by the strokelike episode. We cannot explain conclusively why our findings differ from those reported by neurologists treating adults. If the sites of angiopathy in MELAS most likely include small cerebral arteries, arterioles, and capillaries, small infarcts would be expected rather than the large confluent region of infarction described in many reports of MELAS. L-Arginine is an important precursor of NOx, which may reduce ischemic damage in the acute phase of focal brain ischemia by increasing microcirculation in the cerebral blood flow. The symptoms improved earliest, and magnetic resonance spectroscopy abnormality was minimal when L-arginine was given during the acute phase of strokelike episodes in MELAS.[10]

We evaluated the effects of oral L-arginine supplementation on long-term occurrence of strokelike episodes. The frequency and severity of clinical symptoms of strokelike episodes decreased without serious adverse effects. Prophylactically treated patients with MELAS have not had major strokelike attacks such as hemiconvulsion and hemiparesis. Headache and teichopsia have occurred.

References

1. Pavlakis SG, Phillips PC, DiMauro S, et al. Mitochondrial myopathy, encephalopathy, lactic acidosis, and strokelike episodes: a distinctive clinical syndrome. Ann Neurol 1984;16:481–488.
2. Koga Y, Ishibashi M, Ueki I, et al. Effects of L-arginine on the acute phase of strokes in three patients with MELAS. Neurology 2002;58: 827–828.
3. Lassen LH, Ashina M, Christiansen I, et al. Nitric oxide synthase inhibition in migraine. Lancet 1997;349:401–402.
4. Boger RH, Bode-Boger SM, Thiele W, Junker W, Alexander K, Frolich JC. Biochemical evidence for impaired nitric oxide synthesis in patients with peripheral arterial occlusive diseases. Circulation 1997;95:2068–2074.
5. Nims RW, Darbyshire JF, Saavedra JE, et al. Colorimetric methods for the determination of nitric oxide concentration in neutral aqueous solutions. Methods Enzymol 1996;268:93–105.
6. Honma M, Satoh T, Takezawa J. An ultrasensitive method for the simultaneous determination of cyclic GMP in small-volume samples from blood and tissue. Biochem Med 1977;18:257–273.
7. Piatti PM, Fragasso G, Monti LD, et al. Acute intravenous L-arginine infusion decreases endothelin-1 levels and improves endothelial function in patients with angina pectoris and normal coronary arteriograms. Circulation 2003;107:429–436.
8. Gropen TI, Prohovnik I, Tatemichi TK, Hirano M. Cerebral hyperemia in MELAS. Stroke 1994;25:1873–1876.
9. Iizuka T, Sakai F, Suzuki N, et al. Neuronal hyperexcitability in strokelike episodes of MELAS syndrome. Neurology 2002;59:816–824.
10. Kubota M, Sakakihara Y, Mori M, et al. Beneficial effect of L-arginine for stroke-like episode in MELAS. Brain Dev 2004;26:481–483.